



Modelling and Simulation of Seaways in Deep Water for Simulation of Ship Motions

Kevin McTaggart

Defence R&D Canada

Technical Memorandum

DRDC Atlantic TM 2003-190

September 2003

This page intentionally left blank.

Modelling and Simulation of Seaways in Deep Water for Simulation of Ship Motions

Kevin McTaggart

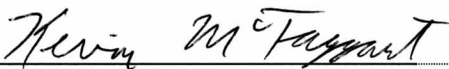
Defence R&D Canada – Atlantic

Technical Memorandum

DRDC Atlantic TM 2003-190

September 2003

Author



Kevin A. McTaggart

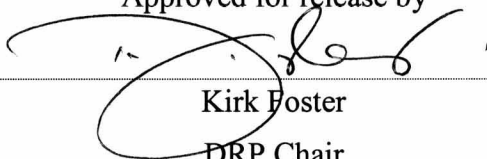
Approved by



Neil Pegg

Head, Warship Performance

Approved for release by



Kirk Foster

DRP Chair

© Her Majesty the Queen as represented by the Minister of National Defence, 2003

© Sa majesté la reine, représentée par le ministre de la Défense nationale, 2003

Abstract

This report presents models of seaways that can be used for simulation of ship motions. The present work assumes deep water, in which ocean wavelengths are less than half the water depth. Seaway models are presented for both regular and random wave conditions, and are given in both fixed and translating axis systems. For regular waves, the nonlinear free surface can be modelled using Stokes second order theory. For both regular and random waves, the influence of the location of the free surface on wave kinematics can be modelled using Wheeler stretching. Commonly used wave spectra and sources of wave climate data are presented as reference information. Sample computations for the frigate HALIFAX illustrate the influence of simulation parameters on predicted RMS motions and required computational time. Required computational time increases significantly when including nonlinear forces from buoyancy and incident waves. In most cases, simulations run faster than real time.

Résumé

Dans ce rapport, nous présentons des modèles de houle pouvant servir à simuler les mouvements de navires. Dans cet article, nous supposons des conditions d'eaux profondes dans lesquelles la longueur d'onde des vagues est inférieure à la moitié de la profondeur. Nous présentons des modèles de houle pour des conditions de vagues régulières et aléatoires, et ces modèles sont données pour des systèmes de coordonnées fixes et en translation. Dans le cas de vagues régulières, on peut modéliser la surface libre non linéaire en appliquant la théorie de Stokes de deuxième ordre. Dans le cas de vagues régulières et aléatoires, on peut modéliser l'effet de l'emplacement de la surface libre sur la cinématique des vagues en utilisant un étalement de Wheeler. Nous présentons à titre d'information de référence les spectres de vagues couramment utilisés et les sources de données sur les vagues. Des calculs échantillons pour la frégate HALIFAX illustrent l'effet des paramètres des simulations sur la valeur quadratique des mouvements prévus et sur le temps de calcul nécessaire. Le temps de calcul nécessaire augmente considérablement lorsqu'on inclut les forces non linéaires associées à la flottabilité et aux vagues incidentes. Dans la plupart des cas, les simulations sont plus rapides que le processus simulé en temps réel.

This page intentionally left blank.

Executive summary

Introduction

DRDC Atlantic is developing a new object-oriented library for simulation of ship motions in waves. This report presents models of regular and random seaways that can be used during simulation of ship motions. The present work assumes deep water, in which seaway wavelengths are less than half the water depth.

Principal Results

Models of regular and random seaways have been developed using both fixed and translating coordinate systems. The relationship between wave phases for fixed and translating coordinate systems is presented. For regular waves, the nonlinear free surface can be modelled using Stokes second order theory. For both regular and random waves, the influence of the location of the free surface on wave kinematics can be modelled using Wheeler stretching. Sample motion computations for the frigate HALIFAX indicate that required computational time increases significantly when including nonlinear forces from buoyancy and incident waves. In most cases, inclusion of nonlinear buoyancy and incident wave forces has little influence on predicted RMS motions.

Significance of Results

Seaway models are now available for simulation applications such as predicting ship motions and visualizing seaways. The presented wave phase relationship between fixed and translating axis systems can be used for applications such as predicting motions of a ship freely maneuvering in a seaway or predicting motions of several ships in a seaway. Presented ship motion predictions typically run faster than real time, indicating they are suitable for real time simulation applications.

Future Plans

Development of DRDC Atlantic's object-oriented ship motion library is continuing. The next phase of work will incorporate forces from rudders, bilge keels, and other appendages into ship motion predictions.

Kevin McTaggart; 2003; Modelling and Simulation of Seaways in Deep Water for Simulation of Ship Motions; DRDC Atlantic TM 2003-190; Defence R&D Canada – Atlantic.

Sommaire

Introduction

RDDC Atlantique est en train d'élaborer une nouvelle base de données orientée objet pour la simulation des mouvements des navires dans la houle. Dans ce rapport, on présente des modèles de houle régulière et aléatoire pouvant servir lors de la simulation des mouvements des navires. Dans la présente étude, on suppose des eaux profondes dans lesquelles la longueur d'onde des vagues est inférieure à la moitié de la profondeur.

Résultats principaux

Nous avons élaboré des modèles de houle régulière et aléatoire, en utilisant des systèmes de coordonnées fixes et en translation. Nous présentons la relation entre les phases des vagues dans ces deux systèmes de coordonnées. Des calculs échantillons de mouvements pour la frégate HALIFAX indiquent que le temps de calcul nécessaire augmente considérablement lorsqu'on inclut les forces non linéaires associées à la flottabilité et aux vagues incidentes. Dans la plupart des cas, l'inclusion de ces forces non linéaires n'a guère d'effet sur la valeur quadratique des mouvements.

Importance des résultats

Nous disposons maintenant de modèles de houle qui permettent de procéder à des simulations comme la prévision des mouvements d'un navire et la visualisation de la houle. La relation, présentée dans cet article, entre les systèmes de coordonnées fixes et en translation qui décrit les phases des vagues peut être utilisée, par exemple, pour prévoir les mouvement de navires qui manœuvrent librement dans la houle ou encore pour prévoir les mouvements de plusieurs navires dans la houle. Les prévisions de mouvement, que nous présentons dans cet article, procèdent normalement plus rapidement qu'en temps réel, ce qui indique qu'elles conviennent aux simulations en temps réel.

Travaux ultérieurs prévus

L'élaboration d'une nouvelle base de données orientée objet sur les mouvements des navires dans la houle se poursuit. Dans la prochaine phase des travaux, nous inclurons dans les prévisions les forces exercées sur le gouvernail, la carène et les autres surfaces.

Kevin McTaggart; 2003; Modelling and Simulation of Seaways in Deep Water for Naval Applications; DRDC Atlantic TM 2003-190; Defence R&D Canada – Atlantic.

Table of contents

| | |
|---|-----|
| Abstract | i |
| Résumé | i |
| Executive summary | iii |
| Sommaire | iv |
| Table of contents | v |
| List of tables | vii |
| List of figures | vii |
| 1 Introduction | 1 |
| 2 Regular Seaways | 1 |
| 2.1 Linear Regular Seaway in Fixed Coordinates | 2 |
| 2.2 Second Order Stokes Theory for Regular Seaway in Fixed Coordinates | 3 |
| 2.3 Regular Seaway in Translating Earth Coordinates | 4 |
| 2.4 Frequency Domain Representation of Regular Seaway in Translating Earth Coordinates | 5 |
| 2.5 Relationships Between Fixed and Translating Earth Coordinate Systems | 7 |
| 2.6 Modelling of Finite Amplitude Wave Kinematics Using Wheeler Stretching | 8 |
| 3 Simulation of Realistic Random Seaways | 8 |
| 3.1 Random Unidirectional Seaway | 9 |
| 3.2 Random Directional Seaway | 9 |
| 3.3 Nonlinear Effects for Random Seaways | 10 |

| | | |
|-------|--|----|
| 4 | Commonly Used Wave Spectral Models | 10 |
| 4.1 | Point Wave Spectra | 10 |
| 4.1.1 | Bretschneider Spectrum | 11 |
| 4.1.2 | Three Parameter JONSWAP Spectrum | 11 |
| 4.1.3 | Ochi and Hubble Six Parameter Spectrum | 12 |
| 4.2 | Directional Wave Spectra | 12 |
| 4.2.1 | Point Spectrum with Cosine Squared Spreading Function | 12 |
| 4.2.2 | Ten Parameter Directional Spectrum | 13 |
| 5 | Wave Climate Data | 13 |
| 6 | Improved Treatment of Nonlinear Buoyancy and Incident Wave Forces | 16 |
| 7 | Numerical Implementation of Seaway Models | 17 |
| 8 | Computational Requirements for Simulating Frigate Motions in Random Seaways | 18 |
| 8.1 | Maximum Recommended Time Step for Accurate Simulations with HALIFAX | 21 |
| 8.2 | Influence of Mesh Size on RMS Motions for HALIFAX | 25 |
| 8.3 | Influence of Nonlinear Forces from Buoyancy and Incident Waves on HALIFAX RMS Motions | 28 |
| 8.4 | CPU Requirements for HALIFAX in Random Seaways | 33 |
| 9 | Influence of Regular Wave Modelling on Ship Motions | 34 |
| 10 | Conclusions | 37 |
| | References | 38 |
| | Symbols and Abbreviations | 41 |
| | Document Control Data | 43 |

List of tables

| | | |
|---|---|----|
| 1 | North Atlantic Wave Scattergram Adapted from Bales et al. for Capsize Risk Analysis | 14 |
| 2 | Main Particulars for HALIFAX Class Frigate, CPF Hydroelastic Model Deep Departure Condition | 19 |
| 3 | Numbers of Panels for Different Panel Meshes | 19 |
| 4 | Ratio of CPU Time to Simulated Time for HALIFAX at 20 knots, Bow Quartering Seas at 150 degrees, Sea State 7, $H_s = 7.5$ m, $T_p = 15.0$ s | 33 |

List of figures

| | | |
|----|---|----|
| 1 | Fixed Coordinate System | 3 |
| 2 | Profiles of Regular Wave at Limiting Steepness $H/\lambda = 0.142$ (no distortion of axes) | 4 |
| 3 | Translating Earth Coordinate System | 6 |
| 4 | Sea Direction Relative to Ship | 6 |
| 5 | Maximum Nominal Wave Steepness Versus Peak Wave Period | 15 |
| 6 | Ship Referenced Coordinate System for Large Angular Motions | 16 |
| 7 | Coarse Mesh for Hull of CPF Hydroelastic Model | 20 |
| 8 | Medium Mesh for Hull of CPF Hydroelastic Model | 20 |
| 9 | Fine Mesh for Hull of CPF Hydroelastic Model | 21 |
| 10 | RMS Motions for HALIFAX from Nonlinear Time Domain Computations with Different Time Steps, Limiting Wave Steepness $\overline{H}/\lambda = 0.049$, 20 knots, Stern Quartering Seas at 30 degrees | 23 |
| 11 | RMS Motions for HALIFAX from Nonlinear Time Domain Computations with Different Time Steps, Limiting Wave Steepness $\overline{H}/\lambda = 0.049$, 20 knots, Bow Quartering Seas at 150 degrees | 24 |

| | | |
|----|--|----|
| 12 | RMS Motions for HALIFAX from Nonlinear Time Domain Computations with Different Meshes, Limiting Wave Steepness $\widetilde{H}/\lambda = 0.049$, 20 knots, Stern Quartering Seas at 30 degrees | 26 |
| 13 | RMS Motions for HALIFAX from Nonlinear Time Domain Computations with Different Meshes, Limiting Wave Steepness $\widetilde{H}/\lambda = 0.049$, 20 knots, Bow Quartering Seas at 150 degrees | 27 |
| 14 | RMS Motions for HALIFAX from Linear and Nonlinear Force Computations, Typical Wave Steepness $\widetilde{H}/\lambda = 0.021$, 20 knots, Stern Quartering Seas at 30 degrees | 29 |
| 15 | RMS Motions for HALIFAX from Linear and Nonlinear Force Computations, Typical Wave Steepness $\widetilde{H}/\lambda = 0.021$, 20 knots, Bow Quartering Seas at 150 degrees | 30 |
| 16 | RMS Motions for HALIFAX from Linear and Nonlinear Force Computations, Limiting Wave Steepness $\widetilde{H}/\lambda = 0.049$, 20 knots, Stern Quartering Seas at 30 degrees | 31 |
| 17 | RMS Motions for HALIFAX from Linear and Nonlinear Force Computations, Limiting Wave Steepness $\widetilde{H}/\lambda = 0.049$, 20 knots, Bow Quartering Seas at 150 degrees | 32 |
| 18 | Heave and Pitch for CPF Hydroelastic Model in Head Seas, $Fn = 0.12$ | 35 |
| 19 | Heave and Pitch for CPF Hydroelastic Model in Head Seas, $Fn = 0.20$ | 36 |

1 Introduction

DRDC Atlantic is developing software components for modelling and simulation of ships in waves. Work completed to date includes predictions of forces and motions in waves for an unappended ship hull in the frequency domain [1] and time domain [2].

This report presents models of seaways that can be used for various simulation applications, including prediction of ship motions and sea loads. Models of regular seaways are useful for comparison of numerical predictions with experimental results, and for computations in the frequency domain. Models of random seaways are useful for modelling realistic sea conditions.

When computing ship motions in waves, it is often convenient to use a translating coordinate system that moves with the forward speed of the ship. This report considers seaway modelling in both fixed and translating coordinate systems, including wave phasing relationships between the two. Correct treatment of wave phasing is necessary for simulation applications such as hull slamming and motions of two ships during replenishment at sea.

The present work is limited to deep seaways, in which the presence of the ocean bottom has no influence on water waves. In practical terms, a seaway can be considered deep when the water depth is greater than half the length of incident waves. Most ship motion predictions, including those in References 1 and 2, are based on the assumption of deep seaways.

Section 2 describes the treatment of regular seaways in both the frequency and time domains. Simulation of realistic random seaways is described in Section 3, followed by descriptions of commonly used wave spectral models in Section 4. Section 5 presents background information on wave climate data relevant for developing simulations. Section 6 presents an improved treatment of rotational moments arising from nonlinear forces due to buoyancy and incident waves. Implementation of seaway models using the Python programming language is described in Section 7. Section 8 describes computational requirements for simulating motions of a frigate in a seaway, and is followed by comparisons between experimental and predicted motions of a frigate in Section 9. Final conclusions are given in Section 10.

2 Regular Seaways

Seaways comprised of regular waves (i.e., waves of a single frequency and direction) are of fundamental importance for ship motion predictions. Motions in random seaways can be evaluated using linear superposition of motion predictions

from regular waves. Due to their repeatability, regular seaways are also important for validation of numerical ship motion predictions using experiments.

Several texts, including Sarpkaya and Isaacson [3] and Chakrabarti [4], give detailed information regarding the theory of regular waves. The present report assumes that the water is sufficiently deep that the ocean bottom does not influence the waves. In practice, bottom effects are negligible when the water depth is greater than half the wavelength.

Regular waves can be considered in various different coordinate systems. It is simplest to consider waves in a fixed coordinate system. A fixed coordinate system is suitable for evaluating loads on fixed structures such as stationary offshore platforms. When considering wave forces acting on a moving object, such as a ship with forward speed, it is more appropriate to treat waves using a moving coordinate system. The present section begins with a treatment using fixed coordinates followed by the more complicated case of a translating coordinate system.

2.1 Linear Regular Seaway in Fixed Coordinates

A regular seaway is most frequently modelled using sinusoidal waves. The application of sinusoidal waves to a seaway is based on the assumption that the wave amplitude is small relative to the wavelength. In the present discussion, incident waves alone are considered, defined as those waves which are not influenced by the presence of a body in the seaway. In reality, the presence of a body such as a ship or offshore structure in a seaway will produce diffracted waves in the vicinity of the body.

Figure 1 shows the fixed coordinate system used for evaluating waves. The waves are travelling from direction ν . The incident wave elevation in fixed coordinates is given by:

$$\zeta_I(x^f, y^f, t) = a \cos \left[k_I (y^f \sin \nu - x^f \cos \nu) - \omega_I t - \epsilon_I^f \right] \quad (1)$$

where a is the wave amplitude, k_I is the incident wavenumber, x_f and y_f are the horizontal plane coordinates, ω_I is the incident wave frequency, and ϵ_I^f is the phase lead angle for the wave crest at the origin. In the present work assuming deep water, the following dispersion relation applies:

$$k_I = \frac{\omega_I^2}{g} \quad (2)$$

where g is gravitational acceleration. The velocity potential and its derivatives are:

$$\Phi_I = \frac{g a}{\omega_I} \sin \left[k_I (y^f \sin \nu - x^f \cos \nu) - \omega_I t - \epsilon_I^f \right] \exp(k_I z_{wl}) \quad (3)$$

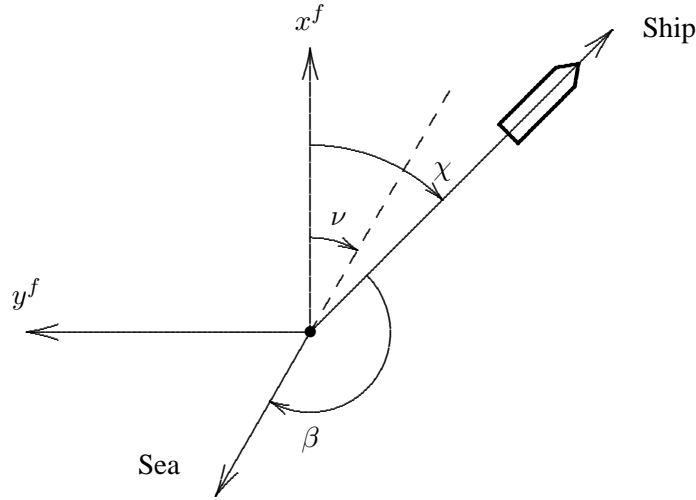


Figure 1: Fixed Coordinate System

$$\frac{\partial \Phi_I}{\partial x^f} = -a \omega_I \cos \nu \cos \left[k_I (y^f \sin \nu - x^f \cos \nu) - \omega_I t - \epsilon_I^f \right] \times \exp(k_I z_{wl}) \quad (4)$$

$$\frac{\partial \Phi_I}{\partial y^f} = a \omega_I \sin \nu \cos \left[k_I (y^f \sin \nu - x^f \cos \nu) - \omega_I t - \epsilon_I^f \right] \times \exp(k_I z_{wl}) \quad (5)$$

$$\frac{\partial \Phi_I}{\partial z} = a \omega_I \sin \left[k_I (y^f \sin \nu - x^f \cos \nu) - \omega_I t - \epsilon_I^f \right] \exp(k_I z_{wl}) \quad (6)$$

$$\frac{\partial \Phi_I}{\partial t} = -g a \cos \left[k_I (y^f \sin \nu - x^f \cos \nu) - \omega_I t - \epsilon_I^f \right] \exp(k_I z_{wl}) \quad (7)$$

where z_{wl} is the elevation (positive upward) relative to the calm water surface. When applying the above equations, it should be noted that the velocity potential and its derivatives will be zero for locations above the free water surface.

2.2 Second Order Stokes Theory for Regular Seaway in Fixed Coordinates

Various nonlinear models are available which provide improved accuracy for regular seaways, as discussed in References 3, 4 and 5. The most widely used nonlinear wave theory is Stoke's second order theory. In deep water, the wave elevation given

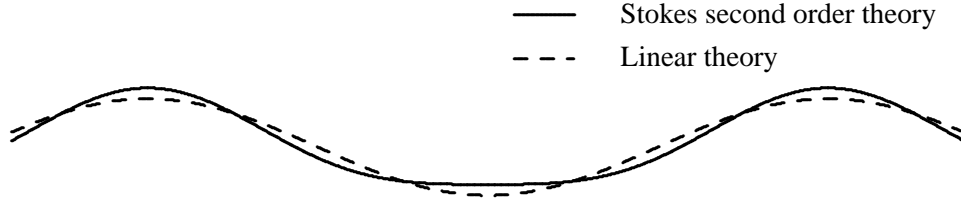


Figure 2: Profiles of Regular Wave at Limiting Steepness $H/\lambda = 0.142$ (no distortion of axes)

by Stoke's second order theory is:

$$\begin{aligned} \zeta_I(x^f, y^f, t) = & a \cos \left[k_I (y^f \sin \nu - x^f \cos \nu) - \omega_I t - \epsilon_I^f \right] \\ & + \frac{a^2 k}{2} \cos 2 \left[k_I (y^f \sin \nu - x^f \cos \nu) - \omega_I t - \epsilon_I^f \right] \end{aligned} \quad (8)$$

For second order Stokes waves in deep water, the velocity potential and its derivatives are the same as for linear theory given in Equations 3 to 7. Similarly the dispersion relation for Stokes second order theory is the same as that for linear theory given in Equation (2).

Due to wave breaking, the maximum possible wave steepness H/λ in deep water is 0.142, where H is wave height and λ is wavelength. Figure 2 gives wave profiles from linear and second order theories at this limiting wave steepness. At lower wave steepnesses, the difference between linear and second order profiles will be less pronounced.

2.3 Regular Seaway in Translating Earth Coordinates

For a ship travelling through a seaway, the forward speed of the ship has a significant influence on the interactions between the ship and the seaway. For example, the frequency of waves encountered by the ship will differ from the incident wave frequency if the ship is travelling with forward speed at any heading other than beam seas. To account for the influence of ship forward speed, ship motion computations are routinely performed in translating earth coordinates. The ship is assumed to travel at steady forward speed and heading, and the coordinate system translates accordingly. Figure 3 shows the translating earth coordinate system and Figure 4 shows the sea direction relative to ship forward speed. The origin of the translating earth coordinate system is located at the ship centre of gravity for the ship in calm water. When evaluating wave kinematics, the vertical coordinate z_{wl} relative to the

calm waterline is used. The following equation relates the relative sea direction to terms of the fixed axis coordinate system presented in Figure 1.

$$\beta = \nu + 180^\circ - \chi \quad (9)$$

where χ is the ship heading relative to the x^f axis.

For linear regular waves, the wave elevation in translating earth axes is given by:

$$\zeta_I(x, y, t) = a \cos[k_I (x \cos \beta - y \sin \beta) - \omega_e t - \epsilon_I] \quad (10)$$

where x and y are horizontal plane coordinates as shown in Figure 3, ω_e is the wave encounter frequency, and ϵ_I is the wave phase lead of the crest at the origin. The wave encounter frequency is given by:

$$\omega_e = |\omega_I - U k_I \cos \beta| \quad (11)$$

where U is the ship forward speed. The wave velocity potential and its derivatives are given by:

$$\Phi_I = \frac{g a}{\omega_I} \sin[k_I (x \cos \beta - y \sin \beta) - \omega_e t - \epsilon_I] \exp(k_I z_{wl}) \quad (12)$$

$$\begin{aligned} \frac{\partial \Phi_I}{\partial x} &= a \omega_I \cos \beta \cos[k_I (x \cos \beta - y \sin \beta) - \omega_e t - \epsilon_I] \\ &\quad \times \exp(k_I z_{wl}) \end{aligned} \quad (13)$$

$$\begin{aligned} \frac{\partial \Phi_I}{\partial y} &= -a \omega_I \sin \beta \cos[k_I (x \cos \beta - y \sin \beta) - \omega_e t - \epsilon_I] \\ &\quad \times \exp(k_I z_{wl}) \end{aligned} \quad (14)$$

$$\frac{\partial \Phi_I}{\partial z} = a \omega_I \sin[k_I (x \cos \beta - y \sin \beta) - \omega_e t - \epsilon_I] \exp(k_I z_{wl}) \quad (15)$$

$$\begin{aligned} \frac{\partial \Phi_I}{\partial t} &= -\frac{g a}{\omega_I} \omega_e \cos[k_I (x \cos \beta - y \sin \beta) - \omega_e t - \epsilon_I] \\ &\quad \times \exp(k_I z_{wl}) \end{aligned} \quad (16)$$

If the regular seaway is modelled using Stokes second order theory, then the wave elevation in translating earth axes is:

$$\begin{aligned} \zeta_I(x, y, t) &= a \cos[k_I (x \cos \beta - y \sin \beta) - \omega_e t - \epsilon_I] \\ &\quad + \frac{a^2 k_I}{2} \cos 2[k_I (x \cos \beta - y \sin \beta) - \omega_e t - \epsilon_I] \end{aligned} \quad (17)$$

2.4 Frequency Domain Representation of Regular Seaway in Translating Earth Coordinates

Ship motions are often computed in the frequency domain using translating earth coordinates, as described in References 1 and 2. Relationships between terms in

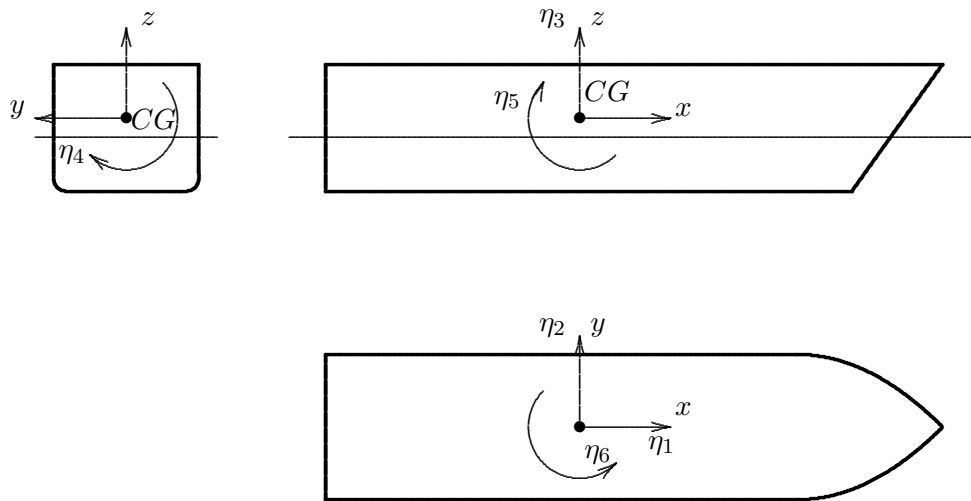


Figure 3: Translating Earth Coordinate System

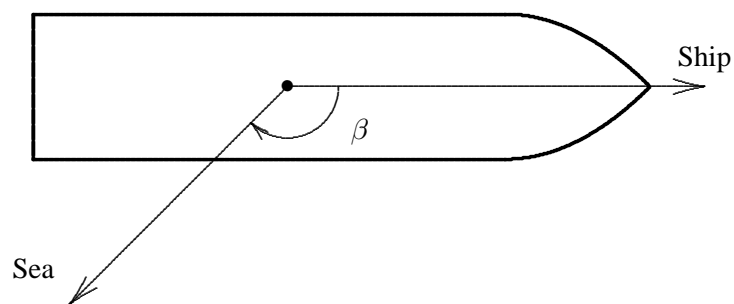


Figure 4: Sea Direction Relative to Ship

the time and frequency domains can be expressed by:

$$\eta_j(t) = \text{Real} \{ \eta_j(\omega_e) \exp(i \omega_e t) \} \text{ for } j = 1 - 6 \quad (18)$$

$$\zeta(t) = \text{Real} \{ \zeta(\omega_e) \exp(i \omega_e t) \} \quad (19)$$

$$\Phi_I(t) = \text{Real} \{ \phi_I(\omega_e) \exp(i \omega_e t) \} \quad (20)$$

where η_j is ship motion displacement for mode j . The frequency domain terms $\eta_j(\omega_e)$, $\zeta(\omega_e)$, and $\phi_I(\omega_e)$ in the above equations are complex quantities which include both amplitude and phase information. For the incident wave velocity potentials given in Equation (20), further distinction between time domain and frequency domain quantities is made by using upper and lower case letters $\Phi_I(t)$ and $\phi_I(\omega_e)$.

Incident wave elevation in the frequency domain is given by:

$$\zeta_I = a \exp[-i k_I (x \cos \beta - y \sin \beta) + i \epsilon_I] \quad (21)$$

The incident wave potential and its derivatives are given in the frequency domain by:

$$\phi_I = \frac{i g a}{\omega_I} \exp[-i k_I (x \cos \beta - y \sin \beta) + i \epsilon_I] \exp(k_I z_{wl}) \quad (22)$$

$$\frac{\partial \phi_I}{\partial x} = a \omega_I \cos \beta \exp[-i k_I (x \cos \beta - y \sin \beta) + i \epsilon_I] \exp(k_I z_{wl}) \quad (23)$$

$$\frac{\partial \phi_I}{\partial y} = -a \omega_I \sin \beta \exp[-i k_I (x \cos \beta - y \sin \beta) + i \epsilon_I] \exp(k_I z_{wl}) \quad (24)$$

$$\frac{\partial \phi_I}{\partial z} = i a \omega_I \exp[-i k_I (x \cos \beta - y \sin \beta) + i \epsilon_I] \exp(k_I z_{wl}) \quad (25)$$

$$\frac{\partial \phi_I}{\partial t} = -\frac{\omega_e g a}{\omega_I} \exp[-i k_I (x \cos \beta - y \sin \beta) + i \epsilon_I] \exp(k_I z_{wl}) \quad (26)$$

2.5 Relationships Between Fixed and Translating Earth Coordinate Systems

Within modelling and simulation applications, it is often useful to be able to shift from a fixed to a translating earth coordinate system. One example is a ship maneuvering in a seaway, whereby many wave-induced force terms are most conveniently evaluated by transformation to translating earth coordinate systems at each time step. If the origin of the translating earth coordinate system is located at x^f, y^f at time t_0 , then the phase lead in translating earth axes will be given by:

$$\epsilon_I = \epsilon_I^f + t_0 (\omega_I - \omega_e) - k_I (y^f \sin \nu - x^f \cos \nu) \quad (27)$$

If the ship is assumed to maintain steady ship speed U and heading ν , then the following relationships will hold:

$$x^f(t) = x^f(t_0) + U (t - t_0) \cos \nu \quad (28)$$

$$y^f(t) = y^f(t_0) - U (t - t_0) \sin \nu \quad (29)$$

$$\frac{\partial \Phi}{\partial x} = \frac{\partial \Phi}{\partial x^f} \cos \chi - \frac{\partial \Phi}{\partial y^f} \sin \chi \quad (30)$$

$$\frac{\partial \Phi}{\partial y} = \frac{\partial \Phi}{\partial y^f} \cos \chi + \frac{\partial \Phi}{\partial x^f} \sin \chi \quad (31)$$

In the context of computing wave forces during simulation of a ship in seaway, the assumption of steady speed and heading will have practical implications. If the ship is assumed to have steady speed and heading, the seaway will require transformation of the seaway from earth-fixed axes to translating earth axes only at the beginning of the simulation. Alternatively, if a simulation models a freely maneuvering ship with speed and heading varying at each time step, then wave force calculations will require transformation of the seaway from earth-fixed axes to translating earth axes at each time step.

2.6 Modelling of Finite Amplitude Wave Kinematics Using Wheeler Stretching

The wave kinematic terms, presented in Equations 3 to 7 for fixed axes and in Equations 12 to 16 for translating axes, are based on the assumption of small amplitude waves. As wave amplitude becomes increasingly large, questions arise regarding the validity of the equations for wave kinematic terms, particularly in the vicinity of the instantaneous water surface. Xu [6] compares various models used for wave kinematic terms in finite amplitude waves. Among the models discussed, Wheeler stretching [7] has been selected here because of its relative simplicity and good agreement with more complicated wave models. In Wheeler stretching, the term $\exp k_I z_{wl}$ is replaced by $\exp k_I (z_{wl} - \zeta(t))$, with $\zeta(t)$ being the instantaneous waterline.

3 Simulation of Realistic Random Seaways

Discussion thus far has been limited to regular waves, limited to a single wave frequency and direction. Realistic seaways consist of wave components arising from many frequencies and directions.

3.1 Random Unidirectional Seaway

Random seaways can be simulated by linear superposition of a finite number of regular wave components. Chakrabarti [4] provides a useful overview of this approach. Using the fixed axis systems of Figure 1, the wave elevation for a unidirectional random seaway can be simulated as follows:

$$\zeta_I(x^f, y^f, t) = \sum_{i=1}^{N_I} a_i \cos \left[k_{I-i} (y^f \sin \nu - x^f \cos \nu) - \omega_{I-i} t - \epsilon_{I-i}^f \right] \quad (32)$$

where N_I is the number of regular wave components used to represent the random seaway, a_i is the wave amplitude for component i , k_{I-i} is the wavenumber for component i , ω_{I-i} is the incident wave frequency for component i , and ϵ_{I-i}^f is the phase for wave component i . The wave amplitude for component i is based on a specified wave spectrum as follows:

$$a_i = \sqrt{2 S_{\omega_I}(\omega_{I-i}) \Delta(\omega_{I-i})} \quad (33)$$

where S_{ω_I} is the spectral density and $\Delta(\omega_{I-i})$ is the wave frequency interval for component i . The wave phase components ϵ_{I-i}^f are obtained using random number generation based on a uniform distribution between 0 and 2π . The following relationship exists between the wave component amplitudes and the standard deviation of water elevation:

$$\sigma^2(\zeta) = \frac{1}{2} \sum_{i=1}^{N_I} a_i^2 \quad (34)$$

The fidelity of the simulated seaway will increase with number of wave components. A minimum of 20 components is typically used for simulating unidirectional random seaways.

Wave kinematic terms for a random seaway are easily determined using summation from regular wave components. When applying Wheeler stretching to wave kinematic terms (Section 2.6), the instantaneous elevation should be evaluated using contributions from all wave components.

3.2 Random Directional Seaway

The simulation of a random directional seaway includes wave components from multiple directions. The following equation is used for modelling the wave surface for a random directional seaway:

$$\zeta_I(x^f, y^f, t) = \sum_{i=0}^{N_I} a_i \cos \left[k_{I-i} (y^f \sin \nu_i - x^f \cos \nu_i) - \omega_{I-i} t - \epsilon_{I-i}^f \right] \quad (35)$$

where ν_i is the direction for wave component i . The amplitude of each wave component is given by:

$$a_i = \sqrt{2 S_{\omega_I, \nu}(\omega_{I-i}, \nu_i) \Delta(\omega_{I-i}) \Delta(\nu_i)} \quad (36)$$

where $S_{\omega_I, \nu}(\omega_{I-i}, \nu_i)$ is the directional spectral density and $\Delta(\nu_i)$ is the direction interval associated with wave component i .

3.3 Nonlinear Effects for Random Seaways

When modelling random seaways, the only nonlinear effect currently modelled is Wheeler stretching, which is applied in the same manner as for regular seas (Section 2.6). Forristall [8] gives an excellent overview of methods for including nonlinear effects in random seaways. It appears that more numerically intensive treatments do not give significantly better results than Wheeler stretching.

4 Commonly Used Wave Spectral Models

The simulation of random seaways described in the previous section requires input wave spectral densities. Wave spectra are typically represented using commonly available models, such as those presented in the SHIPMO7 manual [9]. This section gives some commonly used wave spectral models.

4.1 Point Wave Spectra

Point wave spectra, denoted $S_{\omega_I}(\omega_I)$, give wave spectral energy as a function of wave frequency, and do not include directional information. Point wave spectra are often applied with the assumption that the seaway is unidirectional (i.e., all waves are travelling from the same direction). This assumption is typically more valid in higher sea states, while lower sea states are typically more directionally confused.

The RMS (root-mean-square) wave elevation is related to the wave spectrum by:

$$\sigma(\zeta) = \sqrt{m_0} \quad (37)$$

$$m_i = \int_0^\infty S_{\omega_I}(\omega_I) \omega_I^i d\omega_I \quad (38)$$

where m_i is the i 'th moment for the wave spectrum. A seaway is commonly described in terms of significant wave height H_s , which is the average height of the highest one third of the waves. Assuming a Rayleigh distribution for wave elevation, significant wave height is given by:

$$H_s = 4.005 \sqrt{m_0} \quad (39)$$

The frequency content of a seaway is commonly described using a characteristic wave period, for which several different definitions are available. The peak wave period T_p is the wave period associated with the wave frequency ω_I at which $S_{\omega_I}(\omega_I)$ has its maximum. The average wave period T_1 is another characteristic wave period, and is given by:

$$T_1 = 2 \pi \frac{m_0}{m_1} \quad (40)$$

A third commonly used period is the zero-crossing period given by:

$$T_z = 2 \pi \sqrt{\frac{m_0}{m_2}} \quad (41)$$

4.1.1 Bretschneider Spectrum

The Bretschneider spectrum is the most commonly used model of wave spectra in the open ocean. Based on the 15th International Towing Tank Conference (ITTC) [10], the formulation for the Bretschneider spectrum is:

$$S_{\omega_I}(\omega_I) = \frac{486.0 H_s^2}{T_p^4 \omega^5} \exp \left[\frac{-1948.2}{T_p^4 \omega_I^4} \right] \quad (42)$$

The above spectrum is defined in terms of peak wave period T_p . For a Bretschneider spectrum, the following relations exist with the average and zero-crossing wave periods:

$$T_1 = 0.773 T_p \quad (43)$$

$$T_z = 0.710 T_p \quad (44)$$

4.1.2 Three Parameter JONSWAP Spectrum

The JONSWAP spectrum models relatively high-peaked spectra typically encountered in fetch-limited regions [10]. The JONSWAP spectrum is obtained by multiplying the Bretschneider spectrum by a peak enhancement factor accounting for fetch-limited conditions, giving the following [4]:

$$S_{\omega_I}(\omega_I) = \alpha^* H_s^2 \frac{\omega_p^4}{\omega^5} \exp \left[-1.25 \frac{\omega_p^4}{\omega^4} \right] \gamma^\kappa \quad (45)$$

$$\kappa = \exp \left[\frac{-(\omega - \omega_p)^2}{2\sigma^2 \omega_p^2} \right] \quad (46)$$

$$\sigma = \begin{cases} 0.07 & \text{for } \omega \leq \omega_p \\ 0.09 & \text{for } \omega > \omega_p \end{cases} \quad (47)$$

where ω_p is the peak wave frequency and γ is an input spectral peak parameter. Goda [11] derived the following approximate expression for the normalization term α^* :

$$\alpha^* = \frac{0.0624}{0.230 + 0.0336 \gamma - 0.185/(1.9 + \gamma)} \quad (48)$$

The JONSWAP spectrum is often presented as a two parameter spectrum, with the spectral peak parameter γ having a default value of 3.3.

4.1.3 Ochi and Hubble Six Parameter Spectrum

The Ochi and Hubble 6 parameter spectrum [12] models collinear swell and sea components as follows:

$$S_{\omega_I}(\omega_I) = \frac{1}{4} \sum_{i=1}^2 \frac{\left[\left(\frac{4\lambda_i+1}{4} \right) \omega_{p-i}^4 \right]^{\lambda_i} h_{s-i}^2 \exp \left[- \left(\frac{4\lambda_i+1}{4} \right) \left(\frac{\omega_{p-i}}{\omega} \right)^4 \right]}{\Gamma(\lambda_i) \omega^{(4\lambda_i+1)}} \quad (49)$$

where λ_i , h_{s-i} , and ω_{p-i} are the spectra shape parameter, significant wave height, and peak frequency for component i . The term $\Gamma(\lambda_i)$ is the Gamma function with argument λ_i . If only one of the two components is considered and the shape parameter λ_i equals one, then the six parameter spectrum is equivalent to the Bretschneider spectrum.

4.2 Directional Wave Spectra

The point wave spectra discussed above do not include directional information. To model directionally confused seas, directional wave spectra denoted $S_{\omega_I, \nu}(\omega_I, \nu)$ can be used.

4.2.1 Point Spectrum with Cosine Squared Spreading Function

A directional wave spectrum can be most easily modelled by multiplying a point spectrum by a directional spreading function as follows:

$$S_{\omega_I, \nu}(\omega_I, \nu) = S_{\omega_I}(\omega_I) G(\nu) \quad (50)$$

where $G(\nu)$ is a directional spreading function. Note that the area under the directional spreading function must be unity. A cosine squared spreading function is commonly used, with the following format:

$$G(\nu) = \frac{1}{\gamma_s} \cos^2 \left(\frac{\nu - \bar{\nu}}{\gamma_s} \frac{\pi}{2} \right) \quad \text{for } |\nu - \bar{\nu}| \leq \gamma_s \quad (51)$$

$$G(\theta) = 0 \quad \text{for } |\nu - \bar{\nu}| > \gamma_s \quad (52)$$

where $\bar{\nu}$ is the principal wave direction and γ_s is the spreading angle in radians. A spreading angle of $\pi/2$ (90 degrees) is often used for seakeeping computations.

4.2.2 Ten Parameter Directional Spectrum

Directional seas can be most apparent when sea and swell components are similar in magnitude and are approaching from different directions. The ten parameter spectrum developed by Hogben and Cobb [13] is suitable for modelling such conditions, and has been applied to ship motion predictions by Graham and Juszko [14, 15]. The ten parameter spectrum is a directional extension of the Ochi and Hubble six parameter spectrum, with each of the swell and sea components being multiplied by its own directional spreading function as follows:

$$M_i(\nu) = A(P_i) \cos^{2P_i} \left(\frac{\nu - \bar{\nu}_i}{2} \right) \text{ for } i = 1, 2 \text{ and } |\nu - \bar{\nu}_i| \leq \pi/2 \quad (53)$$

$$M_i(\nu) = 0 \text{ for } i = 1, 2 \text{ and } |\nu - \bar{\nu}_i| > \pi/2 \quad (54)$$

where P_i and $\bar{\nu}_i$ are the directional spread parameter and mean direction (from) for component i . The normalization factor $A(P_i)$ is expressed as:

$$A(P_i) = \frac{2^{(2P_i-1)} \Gamma^2(P_i + 1)}{\pi \Gamma(2P_i + 1)} \quad i = 1, 2 \quad (55)$$

where $\Gamma(2P_i + 1)$ is the Gamma function with argument $2P_i + 1$.

5 Wave Climate Data

Knowledge of wave climatic conditions is generally required for ship motion applications. Such applications can include ship operability analysis [16], analysis of ship structural loads [17], and assessment of ship capsize probabilities [18, 19, 20].

Wave climate data are most commonly presented in the form of scattergrams showing joint probability of occurrence for significant wave height and characteristic wave period (typically peak or zero-crossing wave period). Table 1 shows an example of a wave scattergram for the North Atlantic based on data from Bales et al. [21, 22].

Wave climate data are available from a variety of sources. Bales et al. [21, 22] have published wave scattergrams developed using the Spectral Ocean Wave Model [23], which uses a hindcasting approach based on observed wind data. British Maritime Technology (BMT) Global Wave Statistics [24] is another commonly used data source for wave scattergrams, and is based on visual observations from ships.

Table 1: North Atlantic Wave Scattergram Adapted from Bales et al. [21, 22] for Capsize Risk Analysis

| H_s (m) | 3.2 | 4.5 | 6.3 | 7.5 | 8.5 | 9.7 | 10.9 | 12.4 | 13.9 | 15.0 | 16.4 | 18.0 | 20.0 | 22.5 | 25.7 |
|---------------------------------------|-----|-----|------|------|------|------|------|------|------|------|------|------|------|------|------|
| 0.5 | 541 | 341 | 5488 | 5622 | 3892 | 4861 | 2667 | 2612 | 1180 | 1321 | 592 | 213 | 52 | 4 | |
| 1.5 | | 289 | 3929 | 6631 | 5475 | 5361 | 3627 | 3428 | 1617 | 1707 | 945 | 569 | 164 | 10 | |
| 2.5 | | | 29 | 2150 | 5501 | 5695 | 3829 | 2968 | 1598 | 1267 | 780 | 421 | 124 | 3 | |
| 3.5 | | | | 5 | 822 | 4582 | 3873 | 3393 | 1457 | 1098 | 623 | 350 | 97 | 6 | |
| 4.5 | | | | | 13 | 613 | 3115 | 3381 | 1293 | 1008 | 556 | 316 | 75 | 12 | |
| 5.5 | | | | | | 22 | 631 | 3014 | 1263 | 993 | 467 | 308 | 48 | 5 | |
| 6.5 | | | | | | 2 | 27 | 1336 | 1103 | 934 | 429 | 287 | 40 | | |
| 7.5 | | | | | | | | 229 | 722 | 778 | 347 | 230 | 28 | | 6 |
| 8.5 | | | | | | | | 16 | 218 | 599 | 310 | 200 | 31 | | 7 |
| 9.5 | | | | | | | | 2 | 26 | 187 | 316 | 163 | 20 | 2 | 1 |
| 10.5 | | | | | | | | | 1 | 41 | 202 | 106 | 21 | 1 | |
| 11.5 | | | | | | | | | | 7 | 67 | 95 | 15 | | 1 |
| 12.5 | | | | | | | | | | | 13.5 | 57.5 | 17.5 | | |
| 13.5 | | | | | | | | | | | 13.5 | 57.5 | 17.5 | | |
| 14.5 | | | | | | | | | | | | 13 | 13 | 1.5 | 0.5 |
| 15.5 | | | | | | | | | | | | 13 | 13 | 1.5 | 0.5 |
| 16.5 | | | | | | | | | | | | | 2.5 | 2.5 | |
| 17.5 | | | | | | | | | | | | | 2.5 | 2.5 | |
| 18.5 | | | | | | | | | | | | | | | 0.5 |
| 19.5 | | | | | | | | | | | | | | | 0.5 |
| Total number of observations: 130,339 | | | | | | | | | | | | | | | |

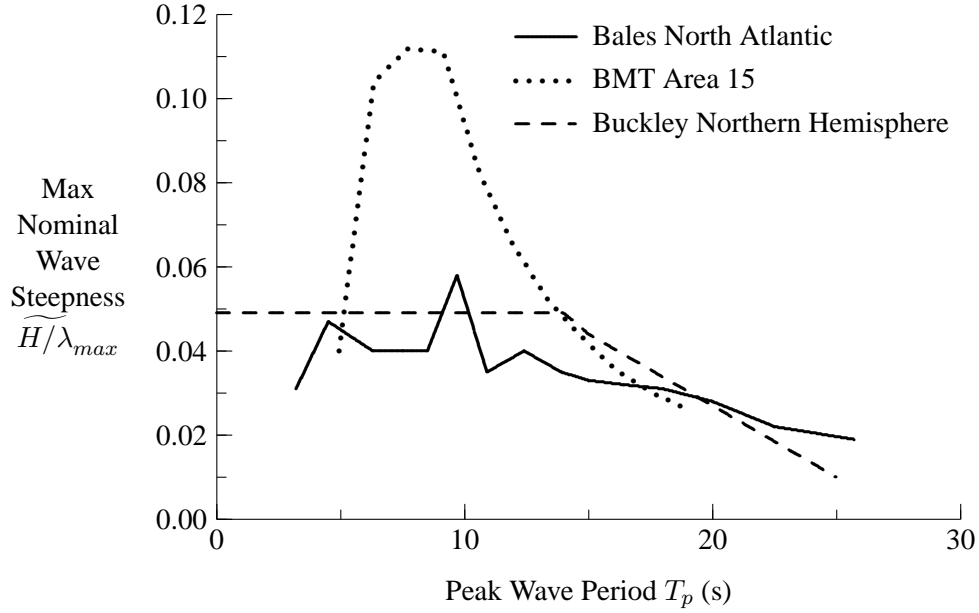


Figure 5: Maximum Nominal Wave Steepness Versus Peak Wave Period

McTaggart and de Kat [19] discuss application of wave climate data from these two different sources to prediction of ship capsizing probabilities in the North Atlantic, and suggest that the BMT data give unrealistically large wave steepnesses. This observation is based on comparison with results from Buckley [25], who used wave buoy observations to develop limiting envelopes of significant wave height versus peak wave period. Buckley's analysis indicates that nominal wave steepness has a limiting value of 0.049, with nominal wave steepness being given by the following for deep water:

$$\widetilde{H/\lambda} = \frac{2 \pi H_s}{g T_p^2} \quad (56)$$

When comparing data from BMT with Buckley's limiting envelope, it should be noted that BMT uses zero-crossing wave period, which can be converted to an equivalent peak wave period using Equation (44). Figure 5 gives maximum nominal wave steepness versus peak wave period using data from BMT, Bales et al., and Buckley's limiting envelope for the Northern Hemisphere. The nominal wave steepnesses based on the BMT data are much steeper than Buckley's limiting envelope. In contrast, the North Atlantic data from Bales give steepnesses which are consistent with Buckley's envelope, with the exception of a single observation of $H_s = 8.5$ m and $T_p = 9.7$ s. The adapted scattergram in Table 1 is based on Bales et al., with the $H_s = 8.5$ m, $T_p = 9.7$ s observation changed to $H_s = 6.5$ m, $T_p = 9.7$ s.

6 Improved Treatment of Nonlinear Buoyancy and Incident Wave Forces

Reference 2 discussed inclusion of nonlinear forces from buoyancy and incident waves when predicting ship motions. These nonlinear forces can be evaluated using direct integrations of pressures over the instantaneous wetted hull surface. The forces are initially evaluated using the ship referenced coordinate system shown in Figure 6, and then transformed to translating earth axes for solution of ship motions.

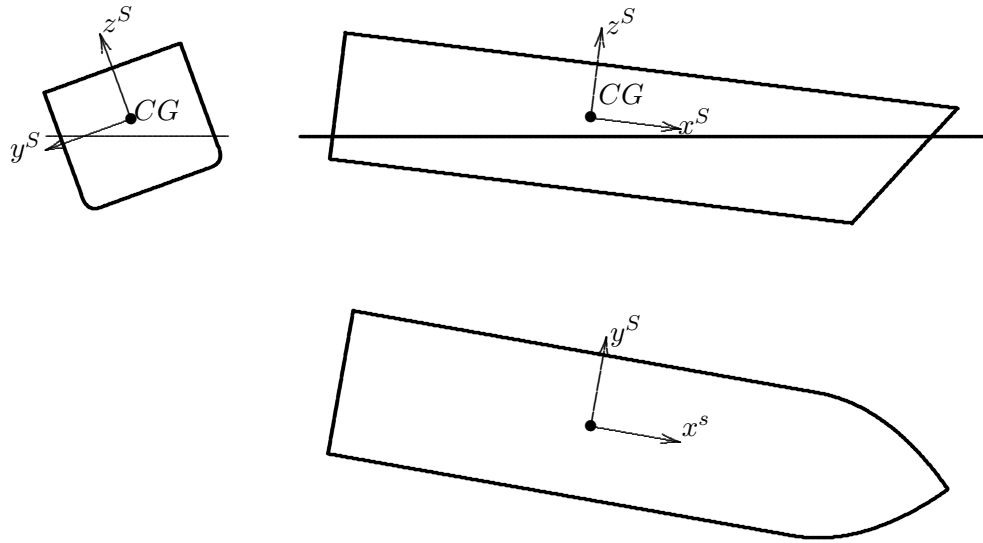


Figure 6: Ship Referenced Coordinate System for Large Angular Motions

Reference 2 gave equations for rotation of translation forces (surge, sway, and heave) from ship-based to translating earth axis systems; however, the transformation of rotational moments (roll, pitch, and yaw) was neglected. For large amplitude ship motions given in translating earth axes, the order of coordinate transformation is yaw, pitch, and roll (i.e., pitch is given relative to the instantaneous ship heading, and roll is given relative to the instantaneous heading and pitch). The complete equations for transforming forces from ship-based to translating earth axis systems are then given by:

$$\begin{aligned} F_1(t) &= F_1^S(t) \cos \eta_6 \cos \eta_5 - F_2^S(t) \sin \eta_6 \cos \eta_5 + F_3^S(t) \sin \eta_5 \quad (57) \\ F_2(t) &= F_1^S(t) (\cos \eta_6 \cos \eta_5 \sin \eta_4 + \sin \eta_6 \cos \eta_4) \\ &\quad + F_2^S(t) (-\sin \eta_6 \sin \eta_5 \sin \eta_4 + \cos \eta_6 \cos \eta_4) \end{aligned}$$

$$- F_3^S(t) \sin \eta_4 \cos \eta_5 \quad (58)$$

$$\begin{aligned} F_3(t) = & F_1^S(t) (-\cos \eta_6 \sin \eta_5 \cos \eta_4 + \sin \eta_6 \sin \eta_4) \\ & + F_2^S(t) (\sin \eta_6 \sin \eta_5 \cos \eta_4 + \cos \eta_6 \sin \eta_4) \\ & + F_3^S(t) \cos \eta_4 \cos \eta_5 \end{aligned} \quad (59)$$

$$F_4(t) = F_4^S(t) \quad (60)$$

$$F_5(t) = F_5^S(t) \cos \eta_4 - F_6^S(t) \sin \eta_4 \quad (61)$$

$$F_6(t) = F_5^S(t) \sin \eta_4 + F_6^S(t) \sin \eta_4 \quad (62)$$

where F_j is the force for mode j in translating earth axes, and F_j^S is the force for mode j in ship-based earth axes.

7 Numerical Implementation of Seaway Models

The seaway models described in Sections 2 and 3 have been implemented using the Python programming language [26, 27] and the Numeric Python library [28]. Four Python classes have been developed to model the following:

- regular seaway in fixed axes,
- regular seaway in translating earth axes,
- random seaway in fixed axes,
- random seaway in translating earth axes.

Each class includes methods in both the time and frequency domains for computing wave elevation, and wave potential and its derivatives. To facilitate efficient computation, the classes exploit the universal function capability of the Numeric library, whereby input coordinates can be provided for a single location or an array of locations when evaluating wave elevation or wave potential.

When computing ship motions using nonlinear wave excitation and buoyancy forces, it is necessary at each time step to determine whether each panel describing the ship hull is below the water. In addition, the pressure on each wetted panel must be determined. These computations require large numbers of evaluations of sine and cosine functions. In an attempt to obtain improved speed performance, functions were developed to evaluate sine and cosine functions using look-up tables. These functions were developed in C and placed in a dynamically linked library (DLL) which could be accessed directly by Python. Unfortunately, the new functions did not give any performance improvement relative to the Numeric library.

New Python functions have been developed to create random unidirectional and multidirectional seaways based on input wave spectra. To improve computational efficiency of time domain computations, these functions remove wave components with negligible fractions of wave energy (e.g., less than one millionth of total wave energy.). When wave components are removed, remaining wave component amplitudes are multiplied by a correction factor to maintain the original energy of the seaway.

8 Computational Requirements for Simulating Frigate Motions in Random Seaways

The computational time required to predict ship motions in a seaway is very important from a practical viewpoint. For training applications, ship motion predictions should run faster than real time. For engineering analysis, it is desirable for ship motion predictions to run significantly faster than real-time to permit examination of large numbers of scenarios.

This section presents some results of simulations for DND's HALIFAX class, with main particulars given in Table 2. The same loading condition was used for simulations in Reference 2. The hull panelling meshes are also the same as for Reference 2. Table 3 gives the number of panels used for the three different meshes, denoted coarse, medium and fine. Figures 7 to 9 show all panels used to represent the ship, including portions below and above the calm waterline. The colour of each panel is a function of elevation relative to the calm waterline.

To ensure coursekeeping during simulations, a supplementary yaw stiffness of 2×10^9 Nm/rad is used, as was done in Reference 2. Note the present work does not consider forces from appendages such as a skeg and rudder, which will contribute to yaw stiffness. Supplementary roll damping of 2×10^7 Nm/(rad/s) represents roll damping from viscous forces and appendage lift, as was done in Reference 2.

Initial simulations for HALIFAX in random seaways revealed excessive surge and sway motions when using nonlinear terms for incident wave forces and buoyancy forces. These excessive motions were due to nonlinear wave drift forces, the lack of stiffness terms for surge and sway, and wave radiation damping approaching zero as wave encounter frequency approaches zero. Wave drift forces arise from non-zero mean force terms that occur when nonlinearities are considered, and have been the subject of extensive research [29, 30, 31, 32]. Chakrabarti [4] provides a useful overview of wave drift forces. To suppress unrealistic surge and sway motions aris-

Table 2: Main Particulars for HALIFAX Class Frigate, CPF Hydroelastic Model
Deep Departure Condition

| | |
|---|---------------------------|
| Length, L | 124.5 m |
| Beam, B | 14.8 m |
| Midships draft, T_{mid} | 4.97 m |
| Trim by stern, t_s | -0.04 m |
| Displacement, Δ | 4655 tonnes (fresh water) |
| Vertical centre of gravity, \overline{KG} | 6.26 m |
| Dry roll radius of gyration r_{xx} | 5.82 m |
| Dry pitch radius of gyration r_{yy} | 28.8 m |
| Dry yaw radius of gyration r_{zz} | 28.8 m |

Table 3: Numbers of Panels for Different Panel Meshes

| | Coarse | Medium | Fine |
|--------------------------------------|--------|--------|------|
| Nominal panel size (m ²) | 5.0 | 2.5 | 1.0 |
| Number of panels on wet hull | 448 | 866 | 2080 |
| Number of panels on dry hull | 824 | 1646 | 3882 |
| Total number of panels | 1272 | 2512 | 5962 |

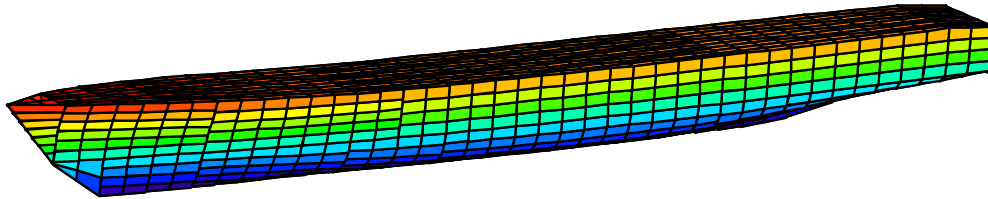


Figure 7: Coarse Mesh for Hull of CPF Hydroelastic Model

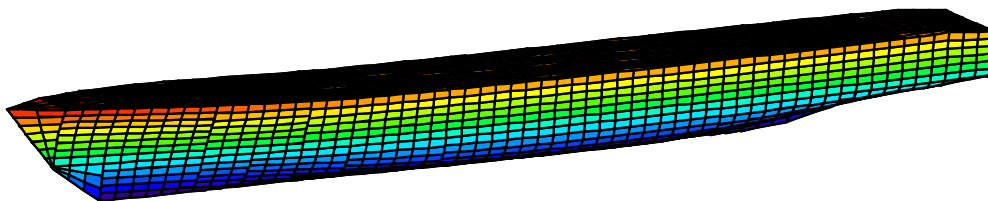


Figure 8: Medium Mesh for Hull of CPF Hydroelastic Model

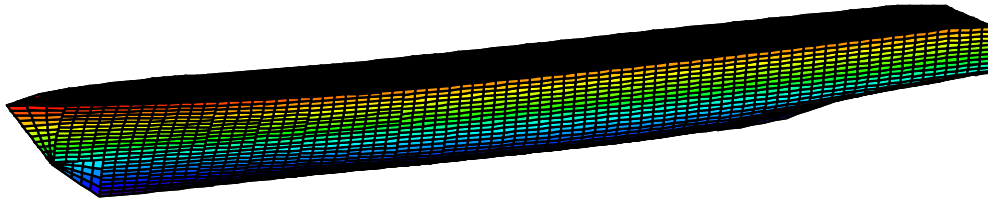


Figure 9: *Fine Mesh for Hull of CPF Hydroelastic Model*

ing from nonlinear wave drift forces, supplementary stiffness and damping terms were used. Finn et al. [33] found it necessary to use this approach in their recent work on ship motions in seaways. When determining suitable values for supplementary stiffness and damping, it was postulated that a natural period of approximately 20 s and a damping ratio (relative to critical damping) of approximately 0.3 would be appropriate for surge and sway modes. For surge, the selected stiffness was 5×10^5 N/m and the selected damping coefficient was 1×10^6 N/(m/s). For sway, the selected stiffness was 1×10^6 N/m and the selected damping coefficient was 2×10^6 N/(m/s). The differences between the values for surge and sway arise from surge having negligible added mass and sway having added mass approaching the mass of the ship. These selected supplementary stiffness and damping values gave simulation results which appeared to be credible. For an actual ship, stiffness and damping for surge and sway could be provided by control systems influencing propeller speed and rudder angle to regulate ship speed and course.

8.1 Maximum Recommended Time Step for Accurate Simulations with HALIFAX

The CPU time required for simulating ship motions is inversely proportional to the time step used during simulations. Consequently, it is important to determine the maximum time step that can be used while still maintaining accuracy in simulations.

Simulations have been conducted to determine the maximum time step that should be used for the frigate HALIFAX. To ensure that the determined maximum recommended time step is conservative, the simulations have been performed under conditions whereby results will be most sensitive to time step size. Both buoyancy and incident wave excitation forces are evaluated using the instantaneous waterline at each time step. Wheeler stretching (Section 2.6) is used for evaluation of wave kinematic terms. Random seaways are modelled using Bretschneider spectra for significant wave heights ranging from 1 to 10 m. The peak wave period of each seaway is based on the limiting nominal wave steepness of 0.049 determined by Buckley [25]. Each modelled seaway has 19 wave components, which have frequencies of 0.2, 0.3, . . . , 2.0 rad/s. HALIFAX is travelling at a moderately high speed of 20 knots in bow and stern quartering seas, and is modelled using the medium mesh of Figure 8.

The predicted RMS motions in Figures 10 and 11 show that time step sizes of 0.1 and 0.2 s give practically identical results. A time step size of 0.5 s gives noticeable differences in bow quartering seas, in which encounter frequencies are greater than for stern quartering seas. It is recommended that a maximum time step size of 0.2 s be used for simulation of HALIFAX motions in waves.

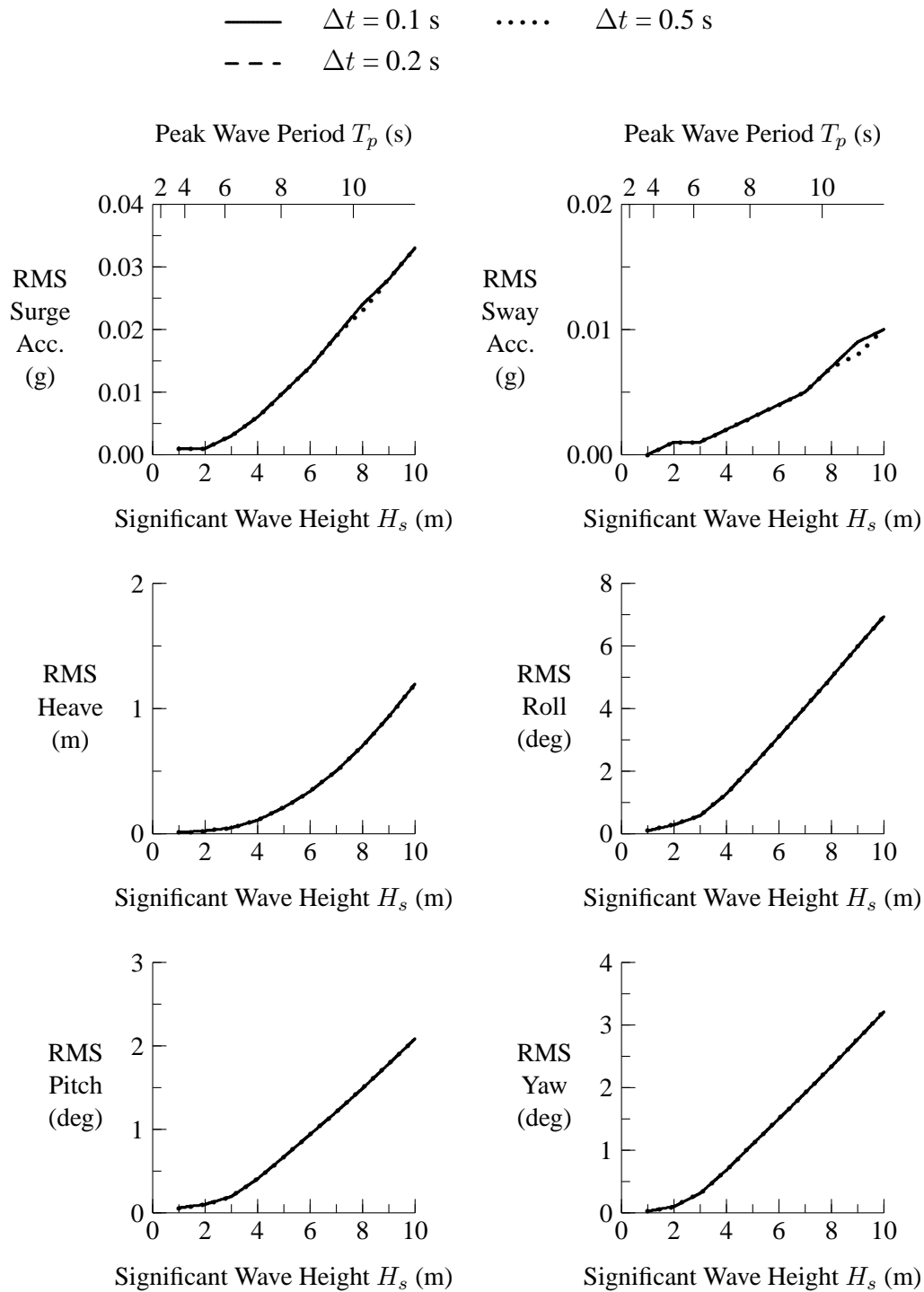


Figure 10: RMS Motions for HALIFAX from Nonlinear Time Domain Computations with Different Time Steps, Limiting Wave Steepness $\widetilde{H}/\lambda = 0.049$, 20 knots, Stern Quartering Seas at 30 degrees

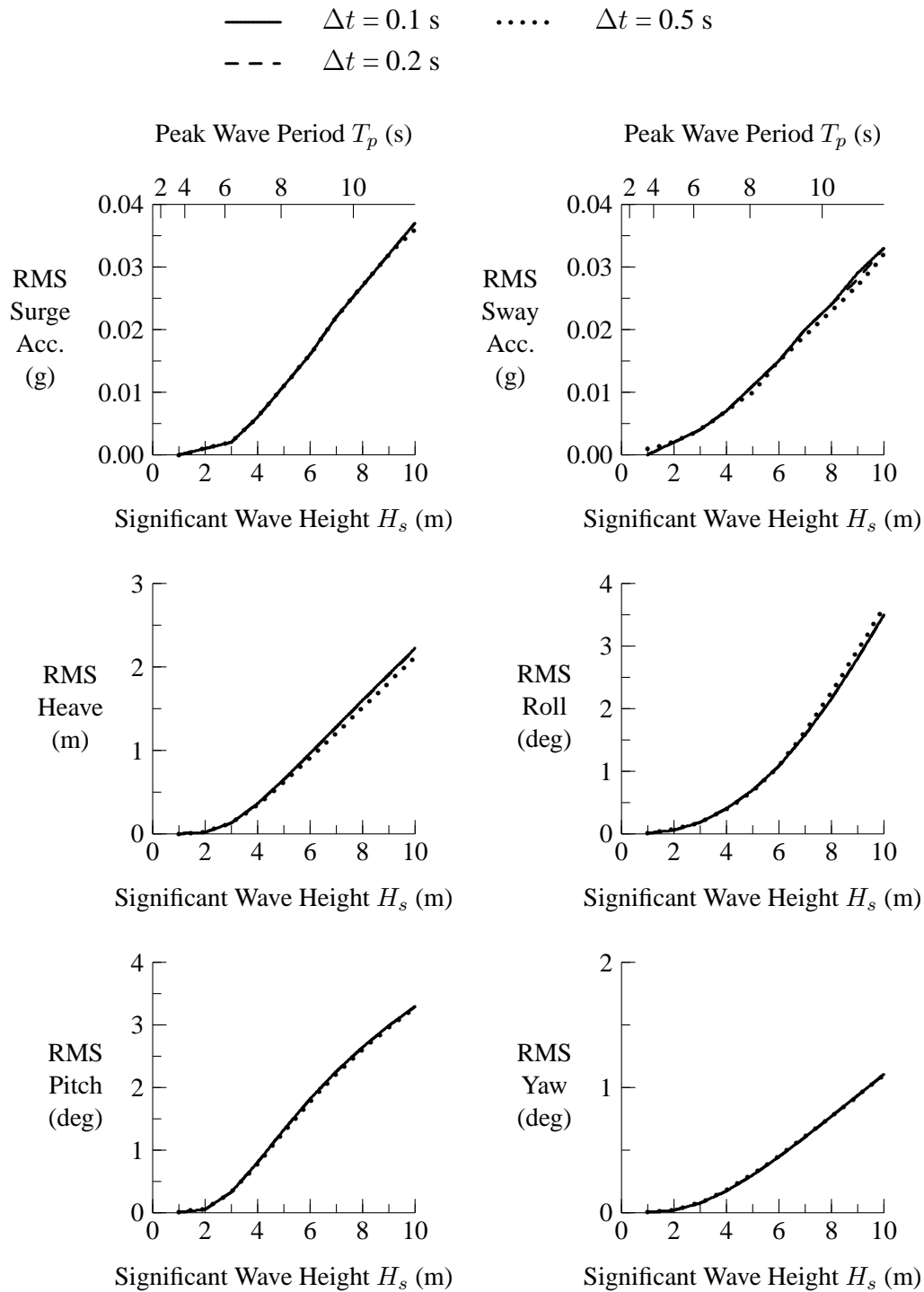


Figure 11: RMS Motions for HALIFAX from Nonlinear Time Domain Computations with Different Time Steps, Limiting Wave Steepness $\widetilde{H}/\lambda = 0.049$, 20 knots, Bow Quartering Seas at 150 degrees

8.2 Influence of Mesh Size on RMS Motions for HALIFAX

When computing ship motions using nonlinear forces from incident waves and buoyancy, the computation time is approximately proportional to the number of panels used to represent the ship hull. Consequently, it is important to know how many panels are required for accurate computation of ship motions. Figures 12 and 13 show RMS motions for HALIFAX in steep waves based on predictions using the three different meshes from Figures 7, 8, and 9. The predictions are based on a time step size of 0.2 s. Predictions using the medium and fine meshes give effectively identical results. Motions predicted using the coarse mesh give slightly different results. The medium mesh appears to give the most suitable balance between accuracy and computation time.

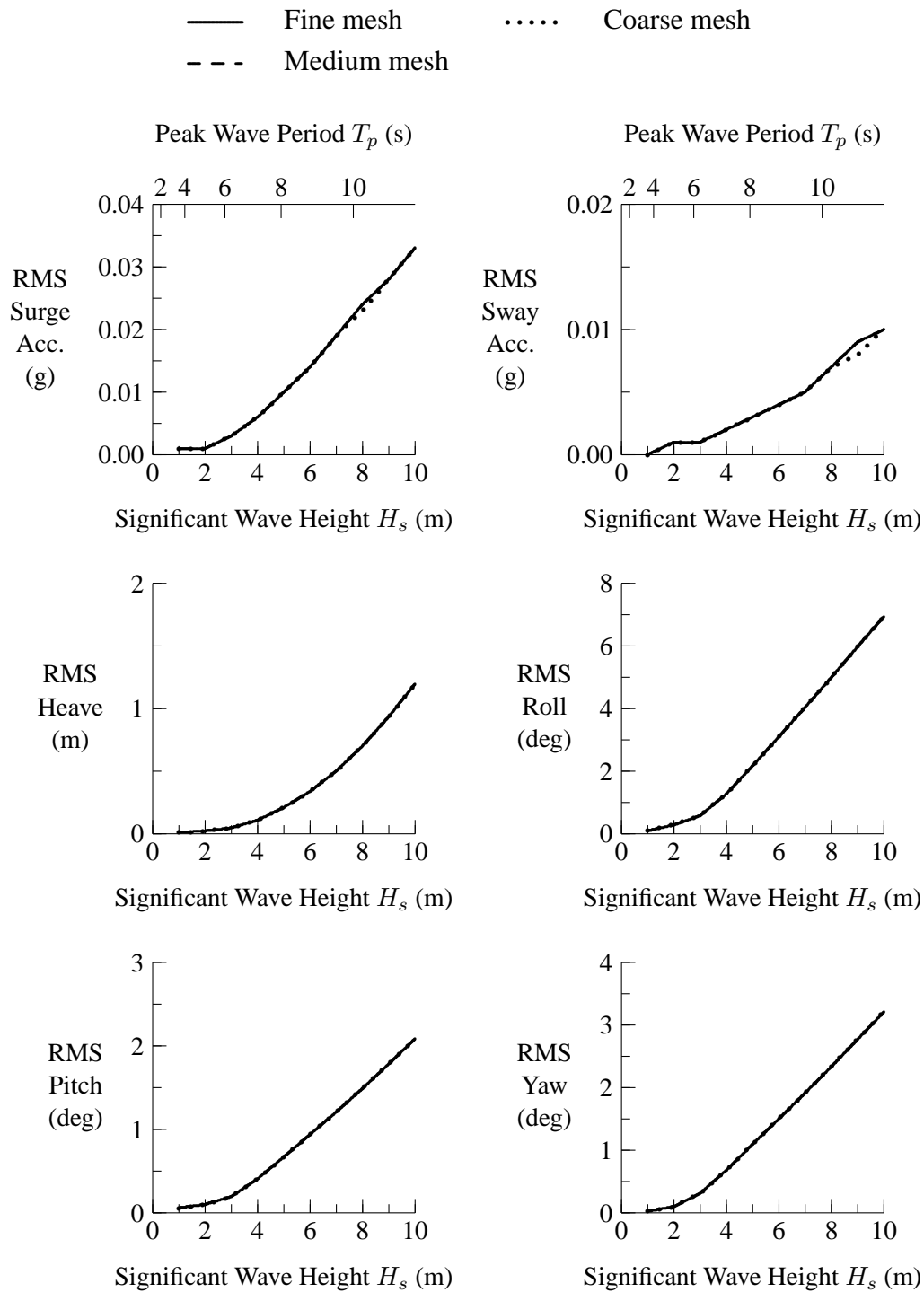


Figure 12: RMS Motions for HALIFAX from Nonlinear Time Domain Computations with Different Meshes, Limiting Wave Steepness $\widetilde{H}/\lambda = 0.049$, 20 knots, Stern Quartering Seas at 30 degrees

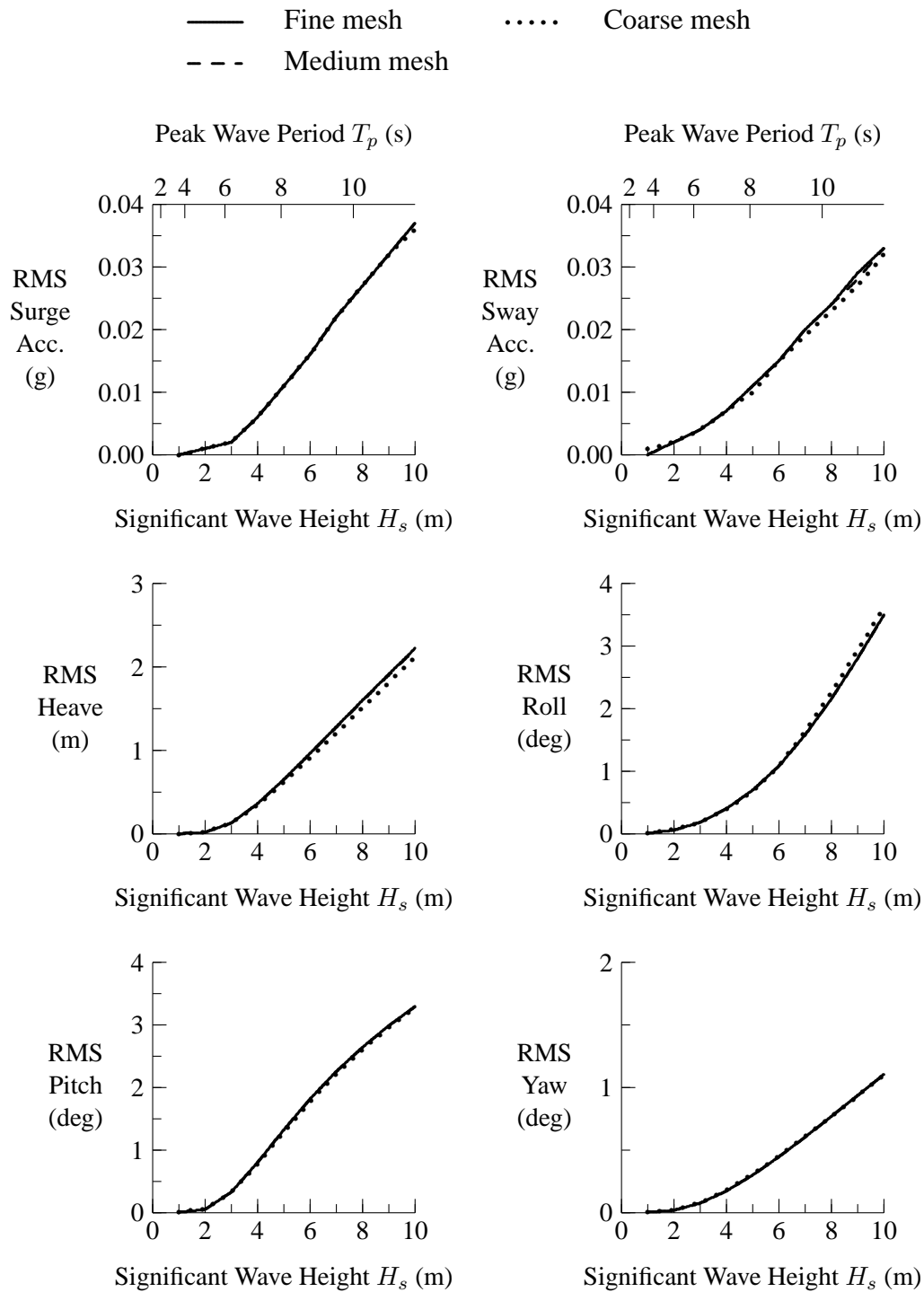


Figure 13: RMS Motions for HALIFAX from Nonlinear Time Domain Computations with Different Meshes, Limiting Wave Steepness $\widetilde{H}/\lambda = 0.049$, 20 knots, Bow Quartering Seas at 150 degrees

8.3 Influence of Nonlinear Forces from Buoyancy and Incident Waves on HALIFAX RMS Motions

Computations using nonlinear forces from buoyancy and incident waves require significantly more time than computations using linear forces; thus, it is important to know under what conditions linear forces can be used. Linear and nonlinear computations were performed using the HALIFAX medium mesh and a time step of 0.2 s.

Figures 14 and 15 show RMS motions for HALIFAX at 20 knots in stern and bow quartering seas in moderate wave steepnesses ($\widehat{H}/\lambda = 0.021$). Force nonlinearities have little influence on ship motions in moderate wave steepnesses, with the exception of roll in bow quartering seas at significant wave heights greater than 3 m. Figures 16 and 17 show the influence of nonlinear buoyancy and incident forces at the limiting wave steepness $\widehat{H}/\lambda = 0.049$. Even in steep waves, force nonlinearities have little influence on ship motions, with the exceptions of roll and yaw in bow quartering seas.

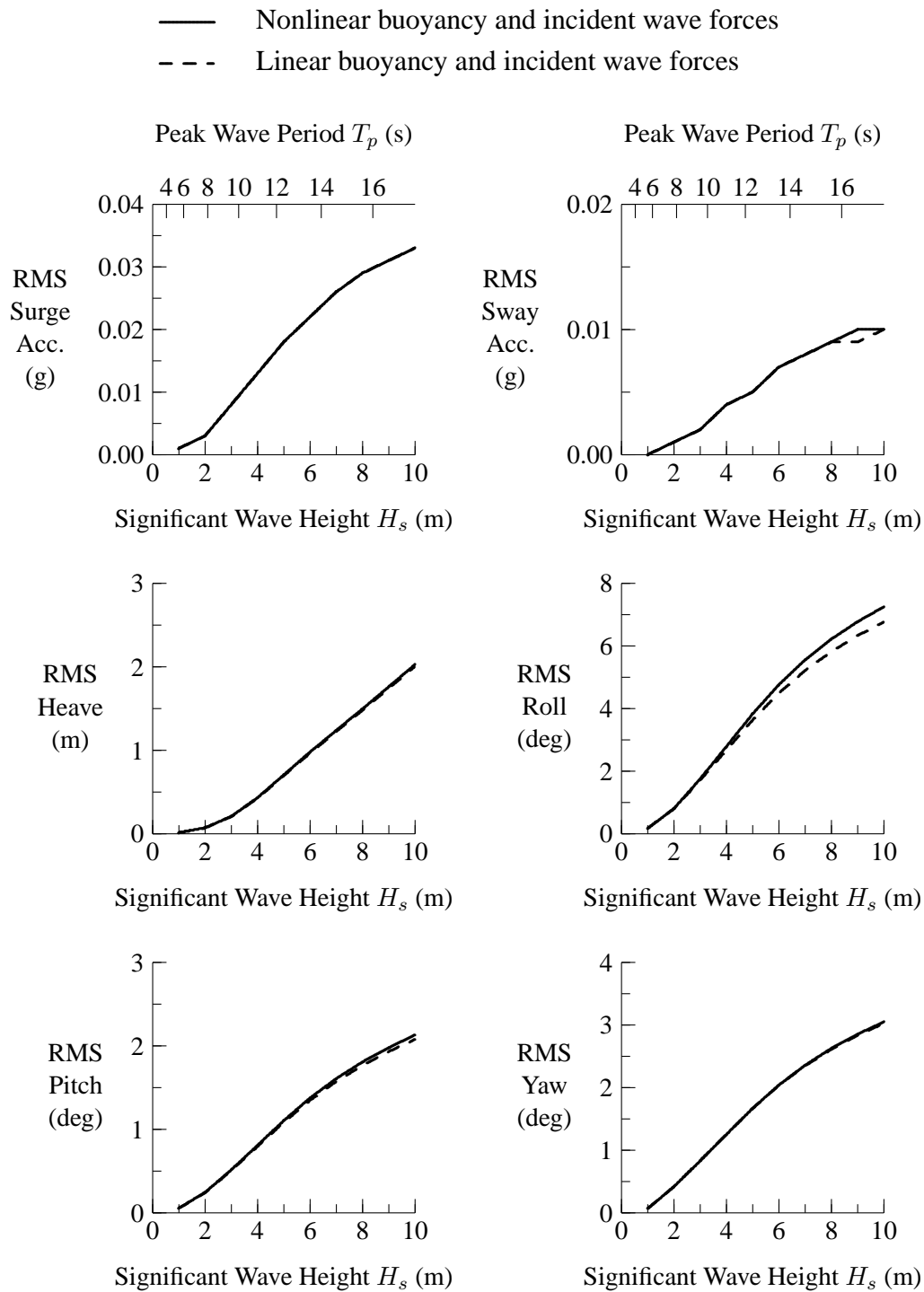


Figure 14: RMS Motions for HALIFAX from Linear and Nonlinear Force Computations, Typical Wave Steepness $\widetilde{H}/\lambda = 0.021$, 20 knots, Stern Quartering Seas at 30 degrees

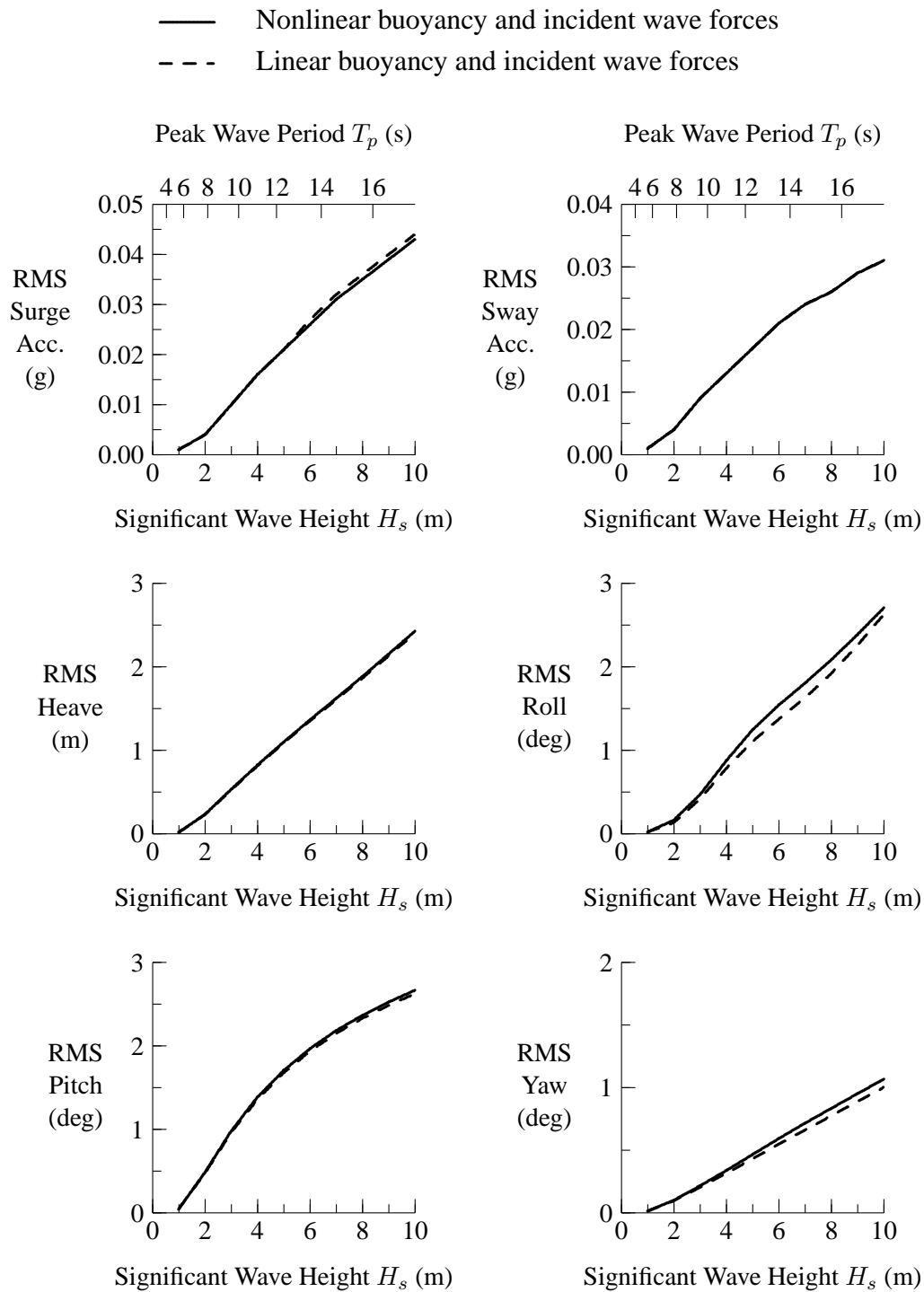


Figure 15: RMS Motions for HALIFAX from Linear and Nonlinear Force Computations, Typical Wave Steepness $\widetilde{H}/\lambda = 0.021$, 20 knots, Bow Quartering Seas at 150 degrees

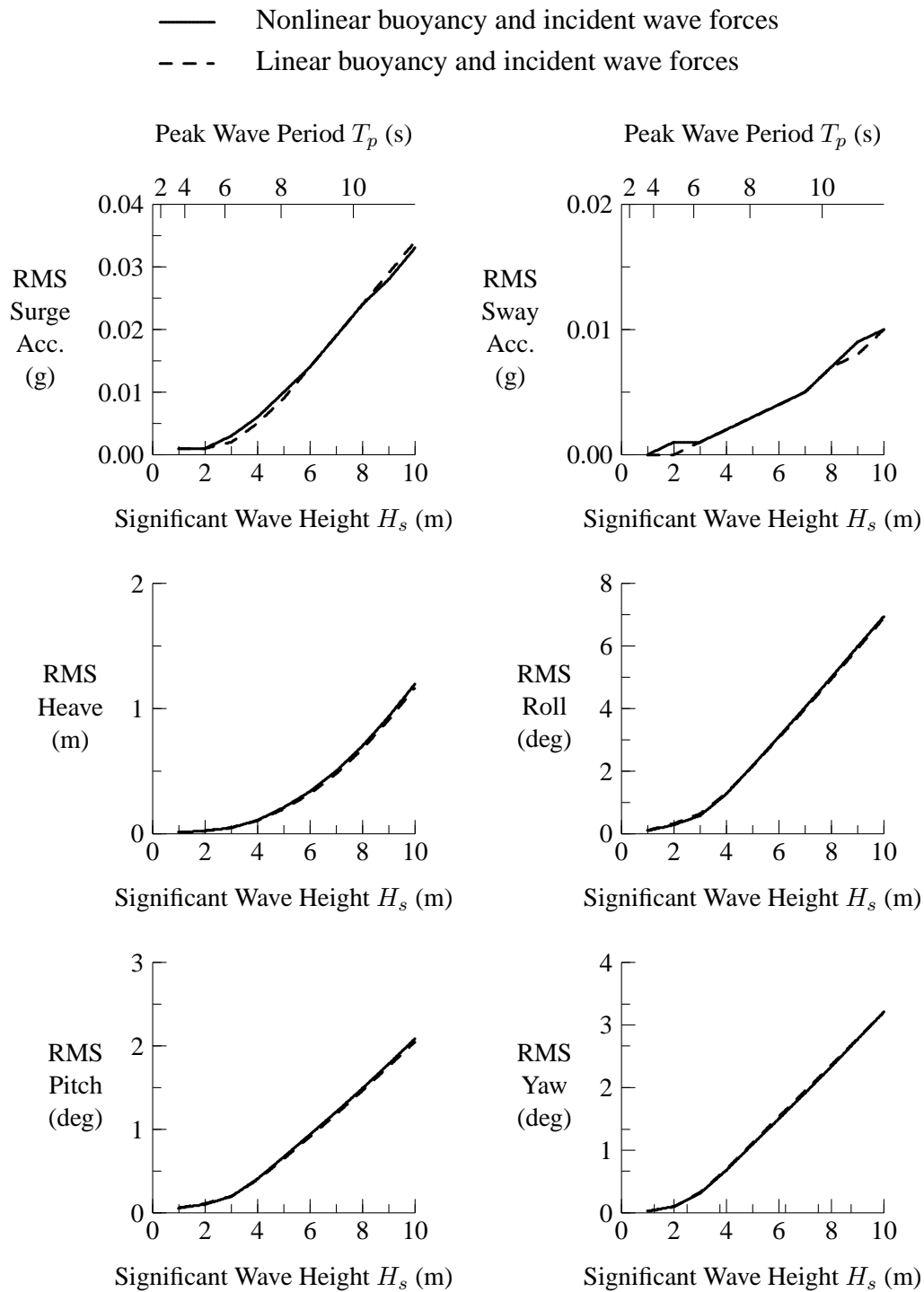


Figure 16: RMS Motions for HALIFAX from Linear and Nonlinear Force Computations, Limiting Wave Steepness $\widetilde{H}/\lambda = 0.049$, 20 knots, Stern Quartering Seas at 30 degrees

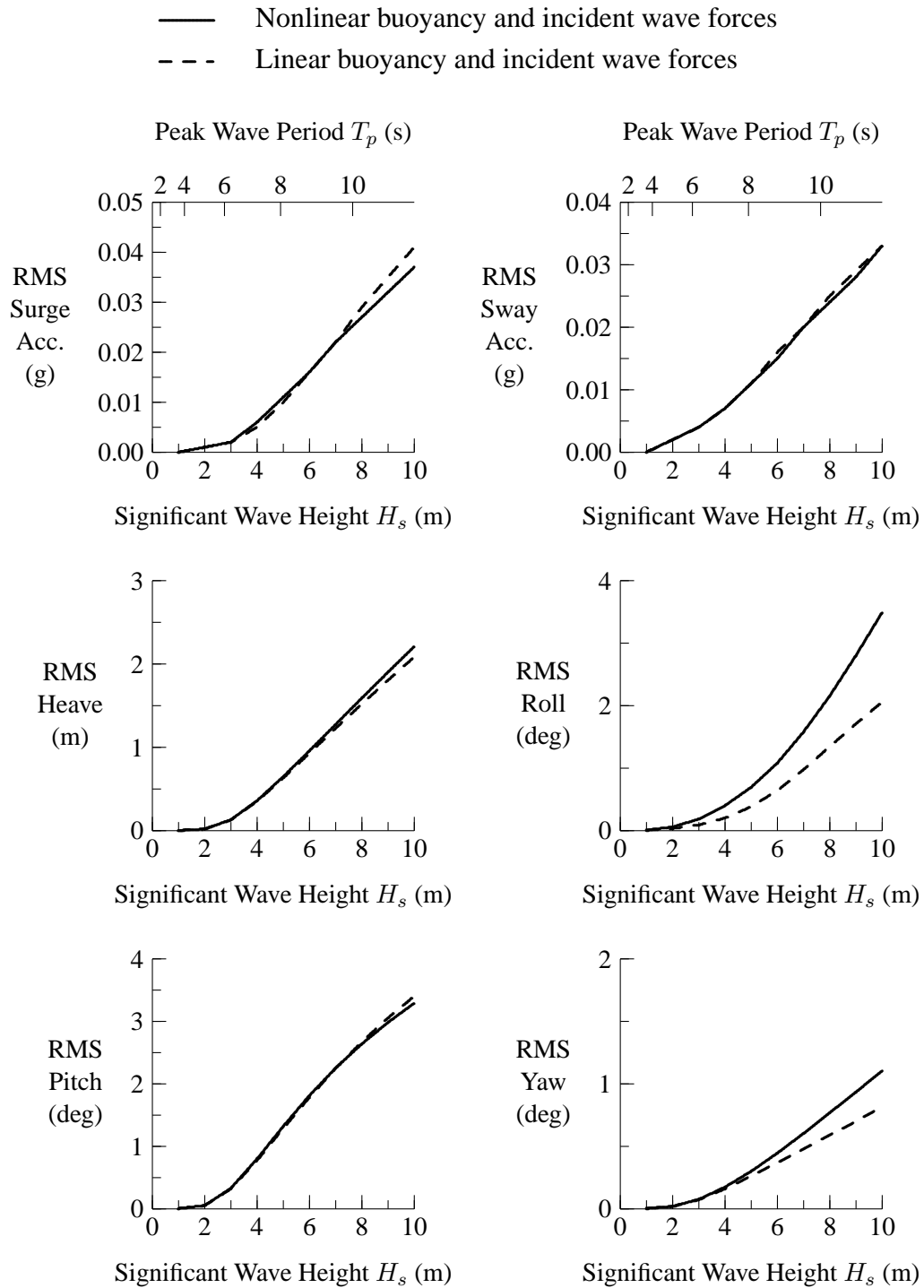


Figure 17: RMS Motions for HALIFAX from Linear and Nonlinear Force Computations, Limiting Wave Steepness $\widetilde{H}/\lambda = 0.049$, 20 knots, Bow Quartering Seas at 150 degrees

8.4 CPU Requirements for HALIFAX in Random Seaways

Required CPU time has been examined for HALIFAX operating in random seaways. Simulations were conducted in NATO sea state 7 ($H_s = 7.5$ m, $T_p = 15.0$ s) in both unidirectional waves and directional waves modelled using a cosine squared spreading function with a spreading angle of 90 degrees. For the unidirectional waves, the seaway was modelled using 19 wave components (0.2, 0.3, . . . , 2.0 rad/s) and 37 wave components (0.2, 0.25, . . . , 2.0 rad/s). For multidirectional waves, 19 wave frequencies and 9 wave directions relative to the mean wave direction (-80, -60, . . . , 80 degrees) were used. In the multidirectional seaway, combinations of wave frequency and sea direction with less than one millionth of the total wave energy were considered negligible and discarded, leaving a total of 160 wave components. A time step size of 0.2 s was used for the simulations.

Table 4 shows the ratio of CPU time to simulated time for the various cases. The simulations using linear buoyancy and incident wave forces run 50 times faster than real time in unidirectional waves. In multidirectional waves, the linear simulations run 12 times faster than real time. The nonlinear simulations using 19 wave components for a unidirectional seaway run 4 times faster than real time.

Table 4: Ratio of CPU Time to Simulated Time for HALIFAX at 20 knots, Bow Quartering Seas at 150 degrees, Sea State 7, $H_s = 7.5$ m, $T_p = 15.0$ s

| Linear or nonlinear buoyancy and incident wave forces | Number of wave components | CPU time/simulated time |
|---|---------------------------|-------------------------|
| Unidirectional waves | | |
| Linear | 19 | 0.019 |
| Nonlinear | 19 | 0.254 |
| Linear | 37 | 0.027 |
| Nonlinear | 37 | 0.435 |
| Multidirectional waves | | |
| Linear | 160 | 0.084 |
| Nonlinear | 160 | 1.636 |

It is useful to consider the above results in the context of various simulation applications. Most ship operations, such as replenishment at sea and helicopter landing, take place in significant wave heights less than 7 m. Under such conditions, differences between linear and nonlinear ship motion predictions are very small;

thus, linear motion simulations can be used with negligible influence on accuracy. In higher sea states (i.e., significant wave heights of 7 m and greater), nonlinear effects can be significant and should be included in simulations for which high fidelity is required. Examples of applications requiring nonlinear predictions include ship capsize, sea loads in high sea states, and helicopter securing in high sea states. Fortunately, directional scattering decreases in higher sea states, and unidirectional seaways can typically be assumed when nonlinear motion predictions are required. It is likely that 19 wave components are sufficient for most ship applications in unidirectional seaways. Given the results in Table 4, ship motion predictions for most applications will run at least 4 times faster than real time.

9 Influence of Regular Wave Modelling on Ship Motions

To illustrate the influence of regular wave modelling on ship motions, numerical predictions using sinusoidal linear waves and Stokes second order waves have been compared with experimental results for the CPF hydroelastic model [34] in head seas. Frequency and time domain predictions use the medium mesh (Figure 8). The time domain predictions for both sinusoidal waves and Stokes second order waves include nonlinear buoyancy and incident wave forces. Wheeler stretching (Section 2.6) is applied when predicting nonlinear incident wave forces. Figures 18 and 19 show that the inclusion of second order wave effects has negligible influence on the motions of the CPF hydroelastic model in head seas.

Figures 18 and 19 show very close agreement between linear frequency domain predictions and time domain predictions including nonlinear forces from buoyancy and incident waves. This result differs from previous comparisons given in Reference 2. The differences between nonlinear time domain predictions from the present and previous studies are due to the introduction of Wheeler stretching in the present work.

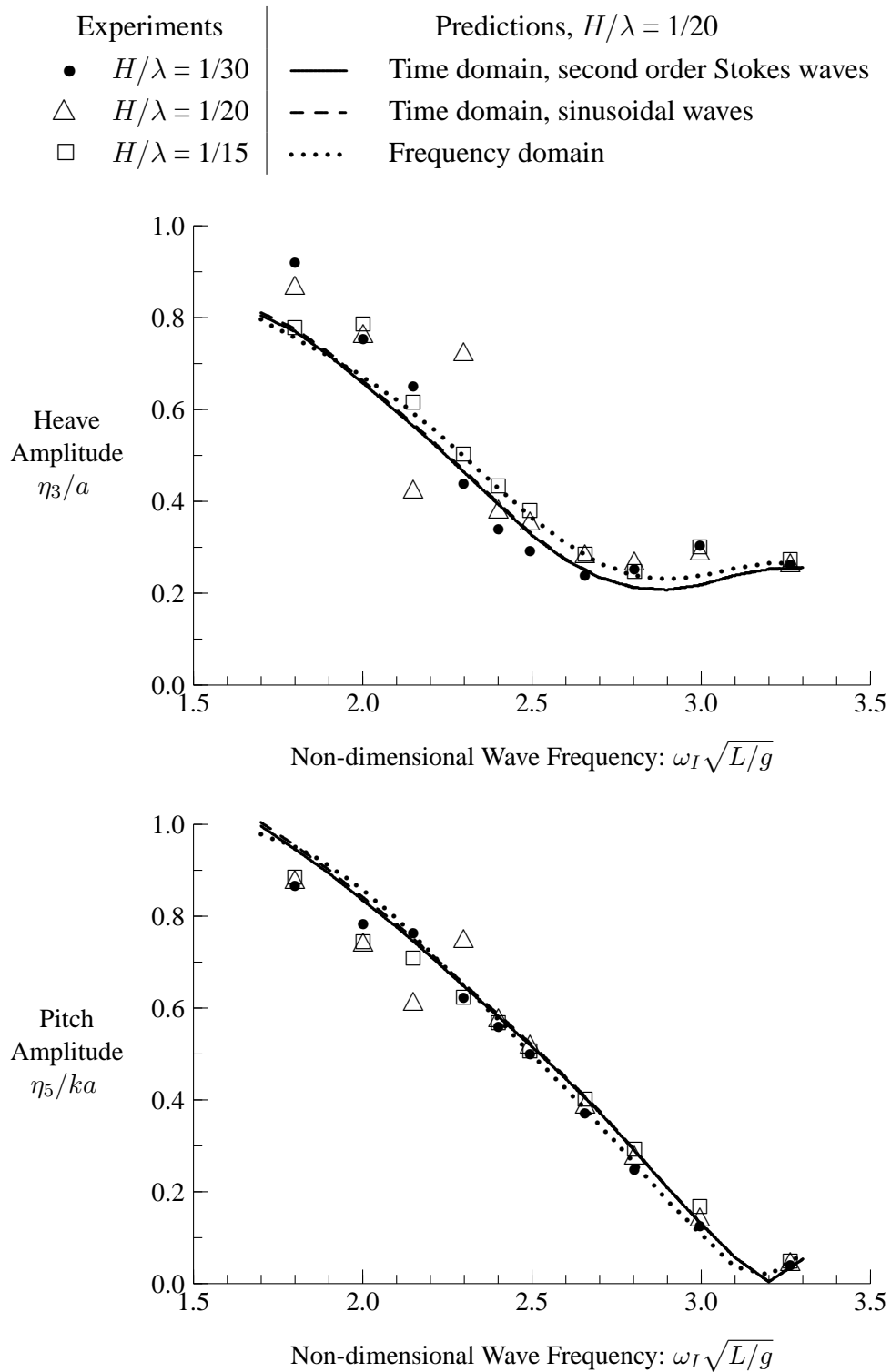


Figure 18: Heave and Pitch for CPF Hydroelastic Model in Head Seas, $F_n = 0.12$

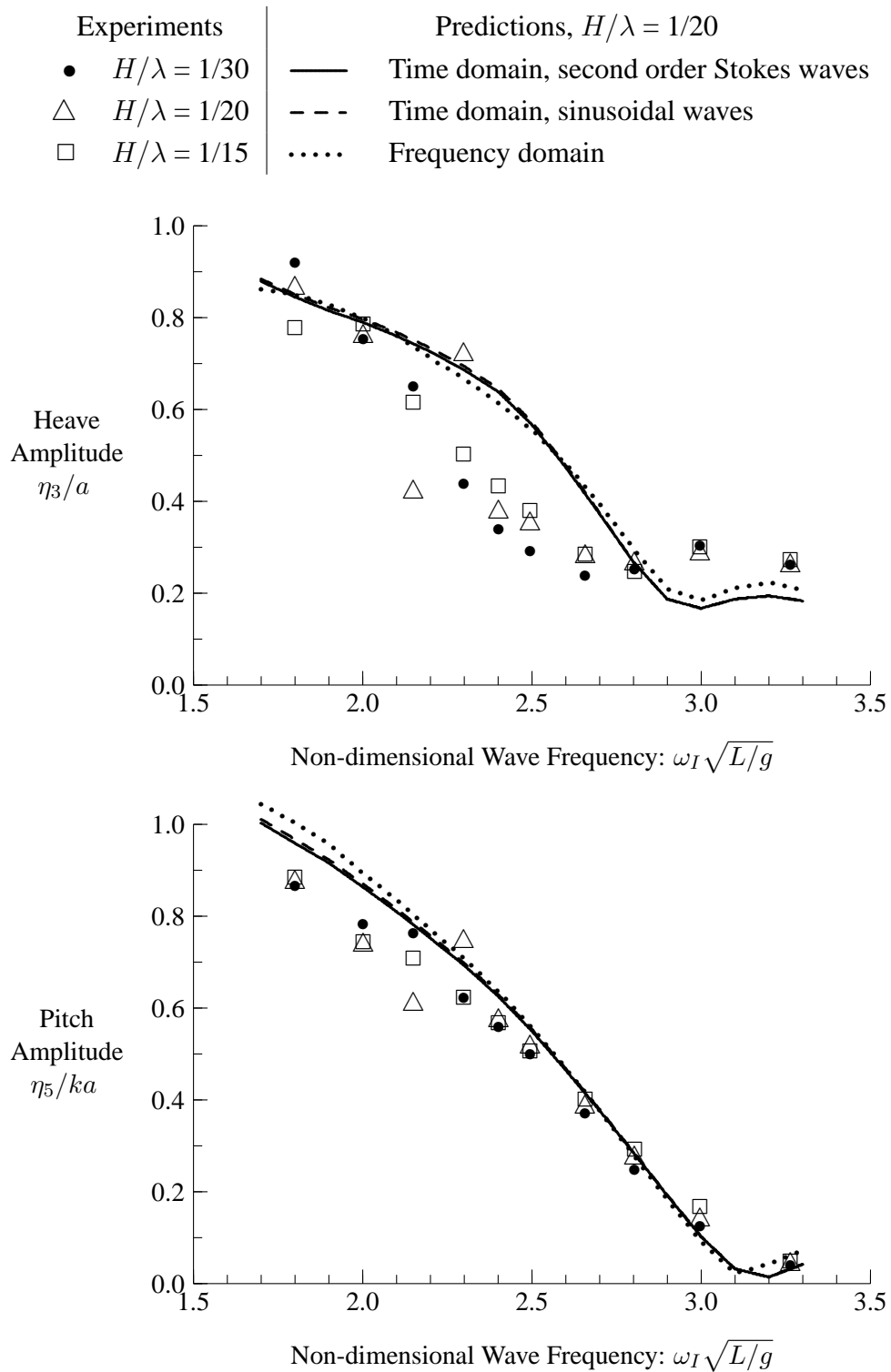


Figure 19: Heave and Pitch for CPF Hydroelastic Model in Head Seas, $F_n = 0.20$

10 Conclusions

Models have been developed for simulating regular and random seaways in both fixed and translating axis systems. Translating axis systems are commonly used for evaluating wave forces on ships. The presented phase relationship between fixed and translating axis systems can be used to ensure consistency of computations and graphically presented results. For regular waves, the nonlinear wave surface can be modelled using Stokes second order theory. The influence of nonlinearities on wave kinematics can be modelled using Wheeler stretching, which can be applied to both regular and random seaways.

Commonly used wave spectral models have been presented. Directional wave effects can be modelled by applying a cosine squared spreading function to a point wave spectrum, or by a ten parameter spectrum, which includes directional terms.

A brief review of wave climate data has discussed available sources. When selecting significant wave height and peak wave period for modelling random seaways, care should be taken to not exceed the limiting nominal wave steepness of 0.049 based on wave buoy observations.

A parametric investigation was performed to investigate sensitivity of RMS motions to the following parameters that significantly influence required computational time: hull panel size, time step size, and usage of linear or nonlinear forces from buoyancy and incident waves. Motions were predicted for HALIFAX at 20 knots in stern quartering and bow quartering random seaways. Computations using different panels sizes show convergence of RMS motions when using a medium mesh with a nominal panel area of 2.5 m^2 , giving 1646 panels on the wet portion of the hull and 2512 panels on the dry portion of the hull. Computations using different time step sizes show good convergence of RMS motions for a time step of 0.2 s. Inclusion of nonlinear forces due to buoyancy and incident waves significantly influences roll and yaw predictions in bow quartering seas. Nonlinear effects are small for other modes in bow quartering seas and for all modes in stern quartering seas.

For simulations in random seaways, the ratio of CPU time to simulated time is highly dependent upon the number of wave components and whether nonlinear forces from buoyancy and incident waves are computed at each time step. Using a 800 MHz Pentium III computer, the ratio of CPU time to simulated time ranged from 0.02 to 1.6.

Comparisons of heave and pitch predictions for HALIFAX with experimental results in regular waves show very good agreement, with nonlinear effects being small.

References

1. McTaggart, K.A. (2002). Three Dimensional Ship Hydrodynamic Coefficients Using the Zero Forward Speed Green Function. (DRDC Atlantic TM 2002-059). Defence Research and Development Canada - Atlantic.
2. McTaggart, K.A. (2003). Hydrodynamic Forces and Motions in the Time Domain for an Unappended Ship Hull. (DRDC Atlantic TM 2003-104). Defence Research and Development Canada - Atlantic.
3. Sarpkaya, T. and Isaacson, M. (1981). *Mechanics of Wave Forces on Offshore Structures*, Van Nostrand Reinhold.
4. Chakrabarti, S.K. (1987). *Hydrodynamics of Offshore Structures*, Springer-Verlag.
5. Newman, J.N. (1977). *Marine Hydrodynamics*, Cambridge, Massachusetts: MIT Press.
6. Xu, H. (1995). Error Analysis of Popular Wave Models for Long-Crested Seas. In *Offshore Technology Conference*, pp. 425–438. Paper OTC 7686, Houston.
7. Wheeler, D.J. (1970). Method for Prediction of Forces Produced by Irregular Waves. *Journal of Petroleum Technology*, pp. 359–367.
8. Forristall, G.Z. (2002). Nonlinear Wave Calculations for Engineering Applications. *Transactions of the ASME, Journal of Offshore Mechanics and Arctic Engineering*, **124**, 28–32.
9. McTaggart, K.A. (1997). SHIPMO7: An Updated Strip Theory Program for Predicting Ship Motions and Sea Loads in Waves. (DREA TM 96/243). Defence Research Establishment Atlantic.
10. (1978). ITTC Seakeeping Committee Report. In *15th International Towing Tank Conference*, Vol. 1, pp. 55–114. The Hague.
11. Goda, Y. (1979). A Review of Statistical Interpretation of Wave Data. (Report 18 (1)). Port and Harbour Research Institute.
12. Ochi, M.K. and Hubble, E.N. (1976). Six-Parameter Wave Spectra. In *15th Coastal Engineering Conference*, Vol. 1, pp. 301–328. Honolulu.
13. Hogben, N. and Cobb, F.C. (1986). Parametric Modelling of Directional Wave Spectra. In *Offshore Technology Conference*, Paper OTC 5212, Houston.

14. Juszko, B.-A. (1989). Parameterization of Directional Wave Spectra - Part 2, Volume I: Final Report. (CR/89/445, Volume I, Juszko Scientific Services). Defence Research Establishment Atlantic.
15. Graham, R. and Juszko, B.-A. (1993). Parameterization of Directional Spectra and Its Influence on Ship Motion Predictions. *Journal of Ship Research*, **37**(2), 138–147.
16. McTaggart, K.A. (2000). SHIPOP2: An Updated Program for Computing Ship Operability in Waves and Wind. (DREA TM 2000-138). Defence Research Establishment Atlantic.
17. McTaggart, K.A. (1998). Prediction of Extreme and Fatigue Sea Loads Using Linear Theory. (TM 98/215). Defence Research Establishment Atlantic.
18. Buckley, W.H. (1998). Ocean Wave Data Required for Use in the Design of Ships. In *Provision and Engineering/Operational Application of Ocean Wave Data*, Paris: World Meteorological Organization.
19. McTaggart, K. and de Kat, J.O. (2000). Capsize Risk of Intact Frigates in Irregular Seas. *Transactions, Society of Naval Architects and Marine Engineers*, Vol. 108.
20. McTaggart, K.A. (2000). Improved Modelling of Capsize Risk in Random Seas. (DREA TM 2000-137). Defence Research Establishment Atlantic.
21. Bales, S.L., Lee, W.T., and Voelker, J.M. (1981). Standardized Wave and Wind Environments for NATO Operational Areas. (Report DTNSRDC/SPD-0919-01). DTNSRDC.
22. Bales, S.L. (1984). Development and Application of a Deep Water Hindcast Wave and Wind Climatology. In *Royal Institute of Naval Architects Wave and Wind Climate World Wide Symposium*, London.
23. Pierson, W.J. (1982). The Spectral Ocean Wave Model (SOWM), A Northern Hemisphere Model for Specifying and Forecasting Ocean Wave Spectra. (Report DTNSRDC/82/011). DTNSRDC.
24. British Maritime Technology Limited (1986). Global Wave Statistics, London: Unwin Brothers.
25. Buckley, W.H. (1994). Stability Criteria: Development of a First Principles Methodology. In *STAB '94, Fifth International Conference on Stability of Ships and Ocean Vehicles*, Vol. 3, Melbourne, Florida.

26. Lutz, M. (2001). *Programming Python*, Second ed. Sebastopol, CA: O'Reilly & Associates.
27. Lutz, M. and Ascher, D. (1999). *Learning Python*, Sebastopol, CA: O'Reilly & Associates.
28. Ascher, D., Dubois, P.F., Hinsen, K., Hugunin, J., and Oliphant, T. (2001). *Numerical Python*. (Technical Report UCRL-MA-128569). Lawrence Livermore National Laboratory. Livermore, California.
29. Havelock, T.H. (1942). Drifting Force on a Ship Among Waves. *Philosophical Magazine*, **33**, 267–475.
30. Maruo, H. (1960). The Drift of a Floating Body in Waves. *Journal of Ship Research*, pp. 1–10.
31. Newman, J.N. (1967). The Drift Force and Moment on Ships in Waves. *Journal of Ship Research*, **11**(1), 51–60.
32. Pinkster, J.A. (1979). Mean and Low Frequency Wave Drifting Forces on Floating Structures. *Ocean Engineering*, **6**, 593–615.
33. Finn, P.J., Beck, R.F., Troesch, A.W., and Shin, Y.S. (2003). Nonlinear Impact Loading in an Oblique Seaway. *Transactions of the ASME, Journal of Offshore Mechanics and Arctic Engineering*, **125**, 190–196.
34. McTaggart, K., Datta, I., Stirling, A., Gibson, S., and Glen, I. (1997). Motions and Loads of a Hydroelastic Frigate Model in Severe Seas. *Transactions, Society of Naval Architects and Marine Engineers*, Vol. 105.

Symbols and Abbreviations

| | |
|--------------------------|--|
| $A(P_i)$ | spectral normalization factor |
| a | wave amplitude |
| a_i | amplitude of wave component i |
| B | beam |
| BMT | British Maritime Technology |
| DLL | dynamically linked library |
| Fn | Froude number |
| $G(\nu)$ | directional spreading function |
| g | gravitational acceleration |
| $\widetilde{H/\lambda}$ | nominal wave steepness |
| H_s | significant wave height |
| h_{s-i} | significant wave height of bimodal spectrum component i |
| \overline{KG} | height of centre of gravity above baseline |
| k_I | incident wavenumber |
| k_{I-i} | incident wavenumber of wave component i |
| L | ship length between perpendiculars |
| $M_i(\nu)$ | directional spreading function of bimodal spectral component i |
| m_i | i 'th moment of spectrum |
| N_I | number of incident wave components |
| P_i | spectral directional spreading parameter |
| RMS | root-mean-square |
| r_{xx} | roll radius of gyration |
| r_{yy} | pitch radius of gyration |
| r_{zz} | yaw radius of gyration |
| $S_{\omega_I}(\omega_I)$ | wave spectral density |
| T_{mid} | draft at midships |
| T_p | peak wave period |
| T_z | zero-crossing period of spectrum |
| T_1 | average wave period |
| t_s | trim by stern |
| t_0 | reference time |
| U | ship forward speed |
| x, y | horizontal plane coordinates in translating earth axes |
| x^f, y^f | horizontal plane coordinates in fixed axes |
| z_{wl} | vertical coordinate relative to calm water surface |
| α^* | normalization factor for JONSWAP spectrum |
| β | wave direction relative to ship |
| γ | peak enhancement factor for JONSWAP spectrum |

| | |
|------------------------|--|
| γ_s | wave spreading angle |
| $\Delta(\omega_{I-i})$ | frequency increment of wave component i |
| ϵ_I | phase lead of incident wave in translating earth coordinate system |
| ϵ_I^f | phase lead of incident wave in fixed coordinate system |
| ϵ_{I-i}^f | phase lead of incident wave component i |
| ζ_I | incident wave elevation |
| η_j | motion displacement in mode j |
| κ | exponent for JONSWAP spectrum |
| λ_i | spectral shape parameter of bimodal spectrum component i |
| ν | wave heading (from) in fixed coordinate system |
| $\bar{\nu}$ | mean wave heading of seaway (from) in fixed coordinate system |
| ρ | water density |
| σ | standard deviation |
| Φ_I | incident wave potential in time domain |
| ϕ_I | incident wave potential in frequency domain |
| χ_I | ship heading (toward) in fixed coordinate system |
| ω_I | incident wave frequency |
| ω_{I-i} | incident frequency of wave component i |
| ω_e | wave encounter frequency |
| ω_p | peak wave frequency |
| ω_{p-i} | peak wave frequency of bimodal spectrum component i |
| Δ | ship mass displacement |

| DOCUMENT CONTROL DATA | | |
|---|---|--|
| (Security classification of title, body of abstract and indexing annotation must be entered when document is classified) | | |
| 1. ORIGINATOR (the name and address of the organization preparing the document). Defence R&D Canada – Atlantic | 2. SECURITY CLASSIFICATION (overall security classification of the document including special warning terms if applicable) UNCLASSIFIED | |
| 3. TITLE (The complete document title as indicated on the title page. Its classification should be indicated by the appropriate abbreviation (S,C,R or U) in parentheses after the title.) Modelling and Simulation of Seaways in Deep Water for Simulation of Ship Motions | | |
| 4. AUTHORS (Last name, first name, middle initial. If military, show rank, e.g. Doe, Maj. John E.) McTaggart, Kevin A. | | |
| 5. DATE OF PUBLICATION (month and year of publication of document) September 2003 | 6a. NO. OF PAGES (total including Annexes, Appendices, etc). 54 | 6b. NO. OF REFS (total cited in document) 34 |
| 7. DESCRIPTIVE NOTES (The category of the document, e.g. technical report, technical note or memorandum. If appropriate, enter the type of report, e.g. interim, progress, summary, annual or final.) Technical Memorandum | | |
| 8. SPONSORING ACTIVITY (the name of the department project office or laboratory sponsoring the research and development. Include address). Defence R&D Canada – Atlantic, PO Box 1012, Dartmouth, NS, Canada B2Y 3Z7 | | |
| 9a. PROJECT OR GRANT NO. (If appropriate, the applicable research and development project or grant number under which the document was written.) 11GK12 | 9b. CONTRACT NO. (if appropriate, the applicable number under which the document was written). | |
| 10a. ORIGINATOR'S DOCUMENT NUMBER (the official document number by which the document is identified by the originating activity. This number must be unique.) DRDC Atlantic TM 2003-190 | 10b. OTHER DOCUMENT NOS. (Any other numbers which may be assigned this document either by the originator or by the sponsor.) | |
| 11. DOCUMENT AVAILABILITY (any limitations on further dissemination of the document, other than those imposed by security classification) (X) Unlimited distribution <input type="checkbox"/> Defence departments and defence contractors; further distribution only as approved <input type="checkbox"/> Defence departments and Canadian defence contractors; further distribution only as approved <input type="checkbox"/> Government departments and agencies; further distribution only as approved <input type="checkbox"/> Defence departments; further distribution only as approved <input type="checkbox"/> Other (please specify): | | |
| 12. DOCUMENT ANNOUNCEMENT (any limitation to the bibliographic announcement of this document. This will normally correspond to the Document Availability (11). However, where further distribution (beyond the audience specified in (11) is possible, a wider announcement audience may be selected). | | |

13. ABSTRACT (a brief and factual summary of the document. It may also appear elsewhere in the body of the document itself. It is highly desirable that the abstract of classified documents be unclassified. Each paragraph of the abstract shall begin with an indication of the security classification of the information in the paragraph (unless the document itself is unclassified) represented as (S), (C), (R), or (U). It is not necessary to include here abstracts in both official languages unless the text is bilingual).

This report presents models of seaways that can be used for simulation of ship motions. The present work assumes deep water, in which ocean wavelengths are less than half the water depth. Seaway models are presented for both regular and random wave conditions, and are given in both fixed and translating axis systems. For regular waves, the nonlinear free surface can be modelled using Stokes second order theory. For both regular and random waves, the influence of the location of the free surface on wave kinematics can be modelled using Wheeler stretching. Commonly used wave spectra and sources of wave climate data are presented as reference information. Sample computations for the frigate HALIFAX illustrate the influence of simulation parameters on predicted RMS motions and required computational time. Required computational time increases significantly when including nonlinear forces from buoyancy and incident waves. In most cases, simulations run faster than real time.

14. KEYWORDS, DESCRIPTORS or IDENTIFIERS (technically meaningful terms or short phrases that characterize a document and could be helpful in cataloguing the document. They should be selected so that no security classification is required. Identifiers, such as equipment model designation, trade name, military project code name, geographic location may also be included. If possible keywords should be selected from a published thesaurus. e.g. Thesaurus of Engineering and Scientific Terms (TEST) and that thesaurus-identified. If it not possible to select indexing terms which are Unclassified, the classification of each should be indicated as with the title).

heave
pitch
ocean waves
seakeeping
ship motions
wave spectra

This page intentionally left blank.

Defence R&D Canada

**Canada's leader in defence
and national security R&D**

R & D pour la défense Canada

**Chef de file au Canada en R & D
pour la défense et la sécurité nationale**



www.drdc-rddc.gc.ca